Emission from international sea transportation and environmental impact

Øyvind Endresen and Eirik Sørgård
Det Norske Veritas, Veritasveien, Høvik, Norway

Jostein K. Sundet, Stig B. Dalsøren, Ivar S. A. Isaksen, and Tore F. Berglen
Department of Geophysics, University of Oslo, Oslo, Norway

Gjermund Gravir
Det Norske Veritas, Veritasveien, Høvik, Norway

Received 30 August 2002; revised 28 March 2003; accepted 10 April 2003; published 13 September 2003.

[1] Emission generated by the international merchant fleet has been suggested to represent a significant contribution to the global anthropogenic emissions. To analyze the impacts of these emissions, we present detailed model studies of the changes in atmospheric composition of pollutants and greenhouse compounds due to emissions from cargo and passenger ships in international trade. Global emission inventories of NO_x, SO_2, CO, CO_2, and volatile organic compounds (VOC) are developed by a bottom-up approach combining ship-type specific engine emission modeling, oil cargo VOC vapor modeling, alternative global distribution methods, and ship operation data. Calculated bunker fuel consumption is found in agreement with international sales statistics. The Automated Mutual-assistance Vessel Rescue system (AMVER) data set is found to best reflect the distributions of cargo ships in international trade. A method based on the relative reporting frequency weighted by the ship size for each vessel type is recommended. We have exploited this modeled ship emissions inventory to estimate perturbations of the global distribution of ozone, methane, sulfate, and nitrogen compounds using a global 3-D chemical transport model with interactive ozone and sulfate chemistry. Ozone perturbations are highly nonlinear, being most efficient in regions of low background pollution. Different data sets (e.g., AMVER, The Comprehensive Ocean-Atmosphere Data Set (COADS)) lead to highly different regional perturbations. A maximum ozone perturbation of approximately 12 ppbv is obtained in the North Atlantic and in the North Pacific during summer months. Global average sulfate loading increases with 2.9%, while the increase is significantly larger over parts of western Europe (up to 8%). In contrast to the AMVER data, the COADS data give particularly large enhancements over the North Atlantic. Ship emissions reduce methane lifetime by approximately 5%. CO_2 and O_3 give positive radiative forcing (RF), and CH_4 and sulfate give negative forcing. The total RF is small (0.01–0.02 W/m^2) and connected with large uncertainties. Increase in acidification is 3–10% in certain coastal areas. The approach presented here is clearly useful for characterizing the present impact of ship emission and will be valuable for assessing the potential effect of various emission-control options. *INDEX TERMS:* 1610 Global Change: Atmosphere (0315, 0325); 1620 Global Change: Climate dynamics (3309); 1630 Global Change: Impact phenomena; 3337 Meteorology and Atmospheric Dynamics: Numerical modeling and data assimilation; *KEYWORDS:* ship emission modeling, ship emission inventories (international shipping), methods and data sets for global distribution of international ship emissions, climate and impact modeling, impacts and climate change related to emissions from international shipping

Citation: Endresen, Ø., E. Sørgård, J. K. Sundet, S. B. Dalsøren, I. S. A. Isaksen, T. F. Berglen, and G. Gravir, Emission from international sea transportation and environmental impact, *J. Geophys. Res.*, *108*(D17), 4560, doi:10.1029/2002JD002898, 2003.

0148-0227/03/2002JD002898

1. Introduction

[2] The world fleet of ocean-going merchant ships above or equal to 100 gross tonnage (GT), representing a typical

Table 1. Distribution of the World Fleet of Ships

Mode	Number of Vessels	Dwt, Millions	GT, Millions	Reference Year
Ocean-going merchant fleet[a] > 100 GT				
All vessels	87,546/84,264		558/508	1996/2000
Cargo fleet	46,205/45,097	792/740	529/482	1996/2000
Noncargo	41,341/39,167		29/26	1996/2000
Inland cargo fleet[b] (waterways)	79,844			1992
Navy fleet[c]				
All vessels[d]	19,646			1995
All vessel > 100 t standard displacement[e]	1338			1998

[a] *LR* [1996, 2000].
[b] *OECD* [1997] (push-towed vessels included).
[c] *Adcock and Stitt* [1995] and *Calhoun* [1999].
[d] Includes 759 submarines.
[e] Includes 523 submarines.

length of above 20–30 m, counts about 85,000 vessels [*Lloyd's Register of Shipping* (*LR*), 1996, 2000]. The fleet can be broadly categorized into 45,000 cargo carrying (general cargo, tankers, container, ferries, etc.) and 40,000 noncargo (research and fishing vessels etc.) vessels. In addition, there are about 40,000 inland waterways vessels (self-propelled) typically of 1000–2000 dead weight tonnage (Dwt) (or approximately 500–1000 GT) [*Organisation for Economic Co-operation and Development* (*OECD*), 1997] and about 1300 large warships above 100 tons (t) standard displacement (or above 300–400 GT) [*Calhoun*, 1999, pp. 280–281]. Table 1 shows the fleet numbers and the tonnage distribution. Ocean-going cargo ships represent the main bulk of the world fleet in terms of GT. Merchant ships in international trade, consuming about 140–150 million tons of bunker fuel (section 3), carry about 5.4 billions of tons of cargo annually [*Fearnleys*, 2002]. Crude oil followed by coal, iron ore, petroleum products, and grains account for roughly 60% of the total international sea-born cargo [*Fearnleys*, 2002]. These principal cargoes are mainly transported in large vessels within a fairly well-defined system of international sea routes (Figures 1–3). Merchant ships in international traffic are subject to International Maritime Organisation (IMO) regulations. Emis-

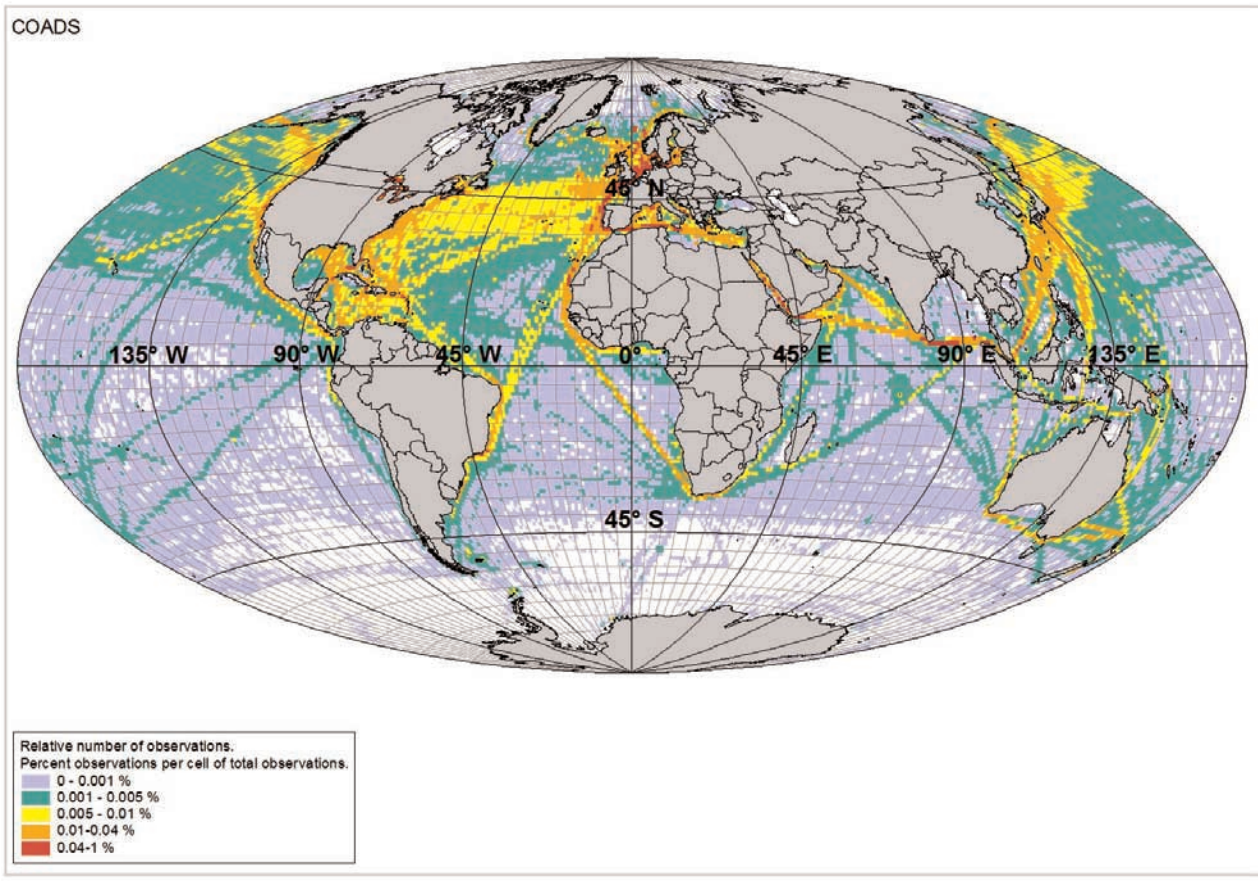

Figure 1. Vessel traffic densities for 1996 based on *COADS* [2001]. The integral over all grid cells equals 1.

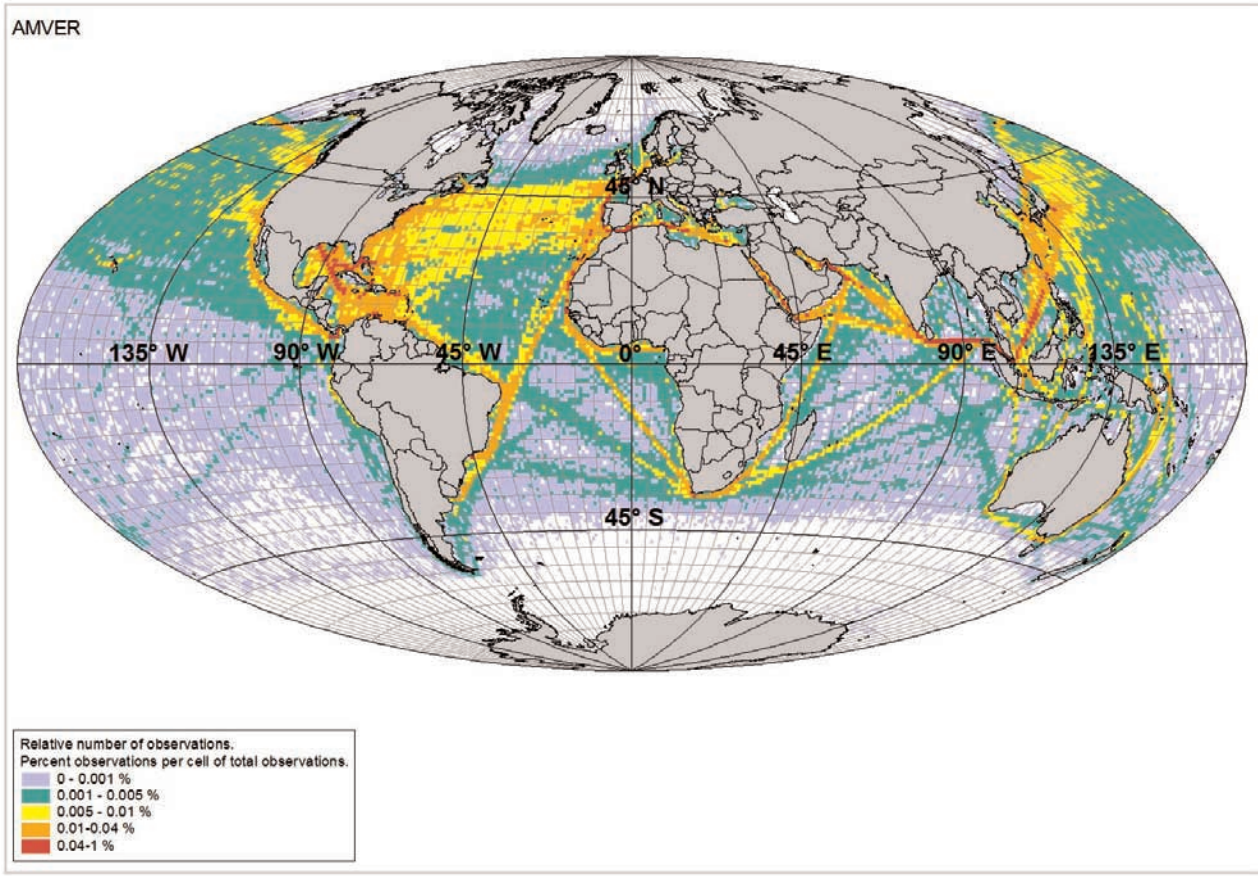

Figure 2. Vessel traffic densities for year 2000 based on the sum of reported distributions from AMVER data (E. Carroll, personal communication, 2001). The integral over all grid cells equals 1.

sions from ships in international trade will be regulated by ANNEX VI of MARPOL 73/78 (the International Convention for the Prevention of Pollution from Ships) [*International Maritime Organisation* (*IMO*), 1998], when it enters into force. The Kyoto agreement does not cover greenhouse gas emissions from ships in international trade (see the United Nations Framework Convention on Climate Change, 2001, available as http://www.unfccc.de/resource/convkp. html).

[3] This paper presents detailed model studies of changes in the atmospheric composition of pollutants and greenhouse compounds due to emissions from cargo and passenger ships in international trade.

[4] Emissions from ships have interrelated environmental impacts. Emission of greenhouse gases changes the radiative balance of the atmosphere. Sulfur and nitrogen compounds emitted from ship will oxidize in the atmosphere to form sulfate and nitrate, and thus contribute to acidification. Emissions of nitrogen oxides, carbon monoxide, and volatile organic compounds (VOC) will lead to enhanced surface ozone formation and methane oxidation, and thus affect the greenhouse warming. Clearly, an integrated study estimating more than one single impact of ship emissions will provide a broader basis to act on when the effect of different emission-control options is considered.

[5] The effect of the international ship emission on the distribution of chemical compounds like NO_x (nitrogen oxides), CO (carbon monoxide), O_3 (ozone), OH (hydroxyl radical), SO_2 (sulfur dioxide), HNO_3 (nitric acid), and sulfate is studied using a global chemical transport model (CTM), the Oslo CTM2. This model has a comprehensive chemical package including the calculation and changes of all the above mentioned compounds. In particular, the large-scale distribution and diurnal variation of the oxidants and sulfur compounds are studied interactively. Meteorological data (winds, temperature, precipitation, clouds, etc.) used as input for the CTM calculations are provided by a weather prediction model.

[6] Several model studies have been performed to study local, regional, and global impacts. *Lawrence and Crutzen* [1999] used a model with high horizontal resolution (192 $\times$ 96 grid boxes) to study how NO_x emissions from ships affect the photochemistry. The distributions of NO_x and ozone and the global-averaged OH concentrations and methane lifetime were calculated, although the results of the calculations were likely affected (as noted by the authors) by the too narrow ship tracks given by the EDGAR 2.0 distribution [*Olivier et al.*, 1996]. Furthermore, oxidation of VOC was not included in the emissions. *Capaldo et al.* [1999] studied the emissions of sulfur compounds using sulfur emissions from ships developed by *Corbett et al.* [1999].

[7] In this article, we first perform new calculations of the fuel consumption and emissions from the international cargo and passenger fleet using a statistical approach

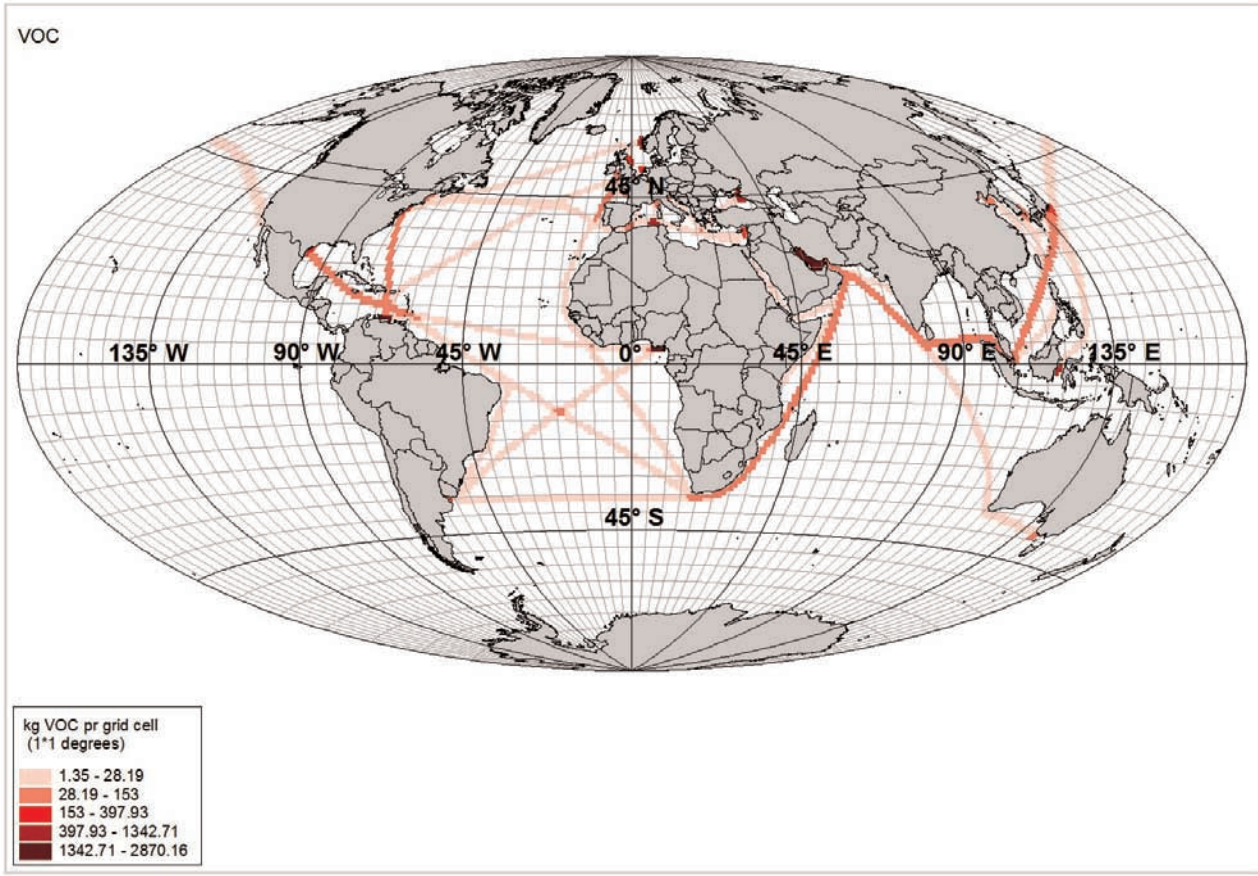

Figure 3. VOC emissions from crude oil transport [*Fearnleys*, 1997, *United Nations*, 1998].

(section 2). These calculations are followed by estimates of bunker fuel consumption for the total world fleet, separated into international and national bunker consumptions (section 3). In section 4 we estimate fuel consumption and the global cargo VOC emissions for large crude oil carriers using fleet and cargo volume movement's data. We also verify the modeling results for large crude oil carriers, with the modeling results present in section 2. Methods and traffic data for global distribution of the emission inventories are discussed in section 5. Calculations of global distribution of key chemical compounds (ozone, CO, NO_x, and sulfate aerosols) and the impacts of the international ship emissions on the distribution of chemical compounds and on radiation balance are calculated in section 6.

2. Modeling of Fuel Consumption and Emissions for the International Cargo and Passenger Fleet

[8] Merchant ships in international traffic are subject to IMO regulations. We have based our calculations on the world fleet statistics of cargo and passenger ships above or equal to 100 GT [*LR*, 1996, 2000]. This will also include some ships not engaged in international voyages and therefore not subjected to IMO regulations, but part of national inventories and the Kyoto agreement.

2.1. Model Description

[9] The emission model estimates fuel consumption and exhaust gas emissions from the main engine(s) for defined ship types [*Endresen and Sørgård*, 1999] (available as http://research.dnv.com/marmil). The fuel consumption module is based on the number of hours at sea (Table 3), statistical relations between size (in Dwt or GT) and engine power for the ship types (container, bulk, general cargo, etc.), distribution of engine types on ship types, bunker fuel consumed per power unit (kW) (Table 2), and an assumed average engine load. (Emission factors per ton fuel are given in Table 4.)

Table 2. Specific Fuel Consumption for Engine Types[a]

Engine Type	Specific Fuel Consumption, kg/kW h
Slow speed	0.195
Medium speed	0.215
High speed	0.230
Turbine machinery	0.290

[a]From *Harrington* [1992] and *Klokk* [1994].

Table 3. Operating Profile in Terms of Operating Hours[a]

Ship Size, Dwt	Number of Hours at Sea Per Year
<5000	4000
5000–100,000	5000
>100,000	6000

[a]From *CONCAWE* [1994], *Norway* [1994], *Liberia* [1996], *Fearnleys* [1997], *Statistics Norway* [2000], Tankerworld (http://www.tankerworld.com/fixtures/fixturesindex.htm).

Table 4. Emission Factors for Gas Compounds Related to Engine Types[a]

Gas Component	Emission Factors for Engine Types, kg emitted per ton fuel			
	Slow Speed	Medium Speed	High Speed	Turbine Machinery
Carbon monoxide (CO)	7.4	7.4	7.4	0.4
Nonmethane volatile organic compounds (NMVOC)	2.4	2.4	2.4	0.1
Methane (CH_4)	0.3	0.3	0.3	0.08
Nitrous oxide (N_2O)	0.08	0.08	0.08	0.08
Carbon dioxide (CO_2)	3170	3170	3170	3170
Sulphur dioxide (SO_2)				
Residual fuel: 2.7% sulphur content	54	54		54
Distillate fuel: 0.5% sulphur content	10	10	10	
Oxides of nitrogen (NO_x)	87	57	57	7
Particulate matter (PM)[b]	7.6	1.2	1.2	2.5

[a]From *E&P Forum* [1993], *LR* [1995], *EMEP/CORINAIR* [1999].
[b]Average estimate with the effect of fuel type taken into account.

[10] The exhaust gas emission is given by:

$$M_{g,i,k,s} = c^f_{g,s} F_{i,k,s} = c^f_{g,s} b_s m_{i,k} t_{i,k} p_{i,k} n_{i,k} e_{i,k,s}, \quad (1)$$

where

$M_{g,i,k,s}$ the amount of pollutant emitted of type g for ships of type i in size category k with engine type s, kg pollution;
$c^f_{g,s}$ the fuel-based emission factor for pollution type g in relation to engine type s, kg pollution/kg fuel;
$F_{i,k,s}$ the fuel consumption of vessels of type i in size category k with engine type s, kg fuel;
b_s the specific fuel consumption for engine type s, kg fuel/kW h;
$m_{i,k}$ the average engine load for a ship of type i and size category k;
$t_{i,k}$ the average number of operating hours during a year for a vessel of type i and size category k, h/yr;
$p_{i,k}$ average installed engine power for a vessel of type i and size category k, kW;
$n_{i,k}$ the number of vessels of type i in size category k;
$e_{i,k,s}$ the fraction of vessels of type i in size category k with engine type s.

[11] Equation (1) is a simplification based on average parameters. Thus interdependencies among the parameters are not taken into account (e.g., emission factors may depend on engine load as given by *Environmental Protection Agency* (*EPA*) [2000], available as http://www.epa.gov/otaq/models/nonrdmdl/c-marine/r00002.pdf). In addition, the emissions will depend on the actual hull shape, the loading condition, the hull roughness, the state of the engine, etc. Auxiliary engines will also contribute to the total exhaust gas emissions, but this is not included in equation 2(1). The different terms in equation (1) are discussed below.

[12] The number of vessels, $n_{i,k}$, above or equal to 100 gross tons in the world fleet is taken from Lloyd's World Fleet Statistics with reference to the years 1996 and 2000 [*LR*, 1996, 2000]. The average installed engine power is correlated with size based on data from 4500 Det Norske Veritas (DNV) classed vessels (SPRINT database), and given by:

$$p_{i,k} = \alpha_i X^{\beta_i}_{i,k}, \quad (2)$$

where α_i and β_i are the regression constants in the equation for ship of type i and $X_{i,k}$ is the average size of ships in size category k of type i. Ship size is given in Dwt for all ship types, except for passenger vessels, where GT is applied. The α_i was found to vary from 2.6 (for container vessels) to 39.8 (for bulk carriers), and β_i varies from 0.5 (for bulk carriers) to 0.86 (for container vessels). The correlation coefficient varied from 0.88 to 0.96 for the different ship types [*Endresen and Sørgård*, 1999]. The average size ($X_{i,k}$) for ship type i with a breakdown on size categories k is based on the World Fleet Statistics [*LR*, 1996, 2000]. The statistical relation given by equation (2) then enables quantification of installed engine power, $p_{i,k}$, and is used in this study.

[13] Data for DNV classed vessels are used to quantify the fraction of engine types, $e_{i,k,s}$, for ship types and class categories. Large ships (above 60,000 Dwt) are usually equipped with slow-speed engines, while for smaller vessels (below 2000 Dwt) the majority have medium-speed engines, though a significant proportion has high-speed engines (about 30%, depending on ship type). Ships between 2000 and 12,000 Dwt are generally equipped with medium-speed engines (about 80%), while ships between 12,000 and 60,000 Dwt are dominated by slow-speed engines (50–80% depending on vessel type). Generally, few ships are equipped with turbine machinery (2–15% of the large ships depending on ship type). The specific fuel consumption for the engine types, b_s, is given in Table 2 [*Harrington*, 1992; *Klokk*, 1994].

[14] The average engine load, $m_{i,k}$, is assumed to be 0.7. In open sea, the ships will usually run the engines on 85% maximum continuous rating (MCR: engine output power available for long periods with nonstop) [*LR*, 1995]. However, periods with slow cruise, port manoeuvring, and ballast cruise reduce the average engine load. We assume an average figure of 70% MCR to be realistic. This corresponds to the average weight load factor of the test cycles defined for main propulsion in the IMO Technical Code, applied for verification of compliance with the NO_x emission limits in accordance with regulation 13 of Annex IV [*IMO*, 1998].

[15] The average activity profile, $t_{i,k}$, for each ship type and size category is given in Table 3. For smaller vessels, the activity profile is mainly based on statistics from Norway (Statistics Norway, 2000, available as http://www.ssb.no/emner/10/12/40/nos_sjofart/arkiv/nos_c582/nos_c582.

Table 5. Modeled Cargo and Passenger Fleet Fuel Consumption and Emissions in 1996 and 2000 From the Main Engine(s) and Auxiliary Engines[a]

	N_2O, kt		NO_x, Mt		CO, kt		NMVOC, kt		PM, kt		SO_2, Mt		CO_2, Mt		Fuel Consumption, Mt	
Ship Type	96	00	96	00	96	00	96	00	96	00	96	00	96	00	96	00
Liquified gas tanker	0.3	0.4	0.3	0.3	27	31	9	10	24	29	0.2	0.2	13	16	4	5
Chemical tanker	0.4	0.5	0.3	0.4	30	39	10	13	25	34	0.2	0.3	14	19	5	6
Oil tanker	2.4	2.4	2.0	2.1	178	185	57	60	172	180	1.4	1.5	93	97	29	31
Bulk ships[b]	2.4	2.4	2.6	2.6	224	226	73	73	222	223	1.6	1.6	96	97	30	30
General cargo[c]	2.1	1.9	1.8	1.7	190	174	62	57	95	113	0.7	0.8	82	75	26	24
Container	1.6	2.3	1.6	2.3	150	214	49	69	124	166	0.9	1.2	64	91	20	29
Ro-Ro ships[d]	0.8	0.8	0.7	0.8	72	76	23	25	33	48	0.2	0.3	31	33	10	10
Passenger vessels	0.3	0.4	0.3	0.4	31	38	10	12	15	21	0.1	0.2	13	16	4	5
Refrigerated cargo	0.3	0.3	0.3	0.3	29	28	9	9	15	15	0.1	0.1	12	12	4	4
Total ME	10.6	11.5	9.8	10.8	931	1010	302	327	726	829	5.5	6.2	419	455	132	144
Total (ME + AUX)	11.7	12.7	10.8	11.9	1024	1111	332	360	799	912	6.1	6.8	461	501	145	158

[a]Values are in Mt (10^6 t) or kt (10^3 t). ME, main engine(s); AUX, auxiliary engines.
[b]Bulk dry and bulk dry/oil vessels.
[c]Including passenger/general cargo vessels.
[d]Including passenger/RO-RO vessels.

pdf) and *CONCAWE* [1994]. The number of operational hours at sea for the larger vessels is mainly based on operational statistics for medium and large bulk and tanker vessels (see *Fearnleys* [1997], available as http://www.fearnleys.com/fearnleys/fearnresearch.htm and Tankerworld (2001), available as http://www.tankerworld.com/fixtures/fixturesindex.htm). The estimated profile seems reasonable for small, medium, and large vessels, considering typical number of voyages per year and time in port. For example, the number of voyages annually is different for large vessels (e.g., crude oil tanker traveling from Arabian Gulf to USA), compared to smaller vessel (e.g., southern North Sea area). The loading/unloading time is port, vessel-type, and size dependent. Typical average time in four ports (excluding ferries) was reported by *CONCAWE* [1994] to vary from 1.5 to 2.4 days (including Rotterdam port) in the southern North Sea area (Lloyd's data). The annual time fraction in port is reported to be 37% for vessels operating in worldwide trade [*Liberia*, 1996], and 59.5% for 605 Norwegian vessels operating in European waters [*Norway*, 1994].

[16] The fuel-based emission factors used in the calculations, c^f_{gs} are summarized in Table 4 and based on the emission factors presented by *Oil Industry International Exploration and Production Forum* [1993], *LR* [1995], and *European Monitoring and Evaluation Programme* (*EMEP*)/*CORINAIR* [1999]. The average sulphur content in marine bunkers is also based on EMEP/CORINAIR recommendations, and is in good agreement with *Cullen* [1997].

2.2. Fuel Consumption and Emissions: Normal Cruising

[17] The modeled main engine(s) fuel consumption and exhaust gas emissions from cargo and passenger vessels above or equal to 100 GT are given in Table 5. Estimates are given with a breakdown on ship types with reference to the years 1996 and 2000. Engine data indicate that installed auxiliary engine power may amount to 45% of main engine power for reefers and passenger vessels. The fraction is lower for other ship types (on the order of 20%). Taking into account the requirements of redundant auxiliary machinery and the average weight load factor of the test cycles defined for auxiliary machinery in the IMO Technical Code [*IMO*, 1998], indicate that fuel consumed by auxiliaries account for 10% of main engine fuel consumption. However, for passenger vessels this estimate (10%) may be too low. A rough estimate may be that the energy consumption by auxiliary engines is on the order of 10% of the main engines consumption. The modeled main engine fuel consumption is 132 Mt in 1996 and 144 Mt in 2000 (Table 5). An additional 10% add-on for auxiliary engines gives an estimate for total fuel consumption of 145 and 158 Mt for 1996 and 2000, respectively.

[18] Global emission data [*Olivier et al.*, 1996] and our ship emission inventories in Table 5, indicate that the emission of CO_2, NO_x, and SO_x by ships corresponds to about 2, 11, and 4% of the global anthropogenic emissions, respectively. These estimates are based on anthropogenic emissions in year 1990 and ship emissions in year 1996, and correspond to results from other studies [*Corbett et al.*, 1999; *Skjølsvik et al.*, 2000]. Emissions from port operations are not included, but this contribution is small as discussed in the next section. The major source of uncertainty in the estimates given above is likely to be related to how anthropogenic emissions may have developed from 1990 to 1996.

2.3. Estimations of Fuel Consumption: Port Operations

[19] The estimates above do not include fuel consumption in port. Important factors influencing in-port consumption are, manoeuvring time, time spent, and cargo operations (vessel-type dependent). In-port emissions seem to range between 2 and 6% of the total emissions, as reported by *Streets et al.* [2000] and *Whall et al.* [2002]. The crude oil transport model described in section 4 estimates fuel consumption for port operations to 9% of the sea transportation consumption, both for medium-sized and large crude oil carriers. Tankers probably have a higher consumption and a rough estimate for the fleet is for port operations a fuel consumption of about 5% of the sea transportation consumption. The additional 5% add-on for port operations

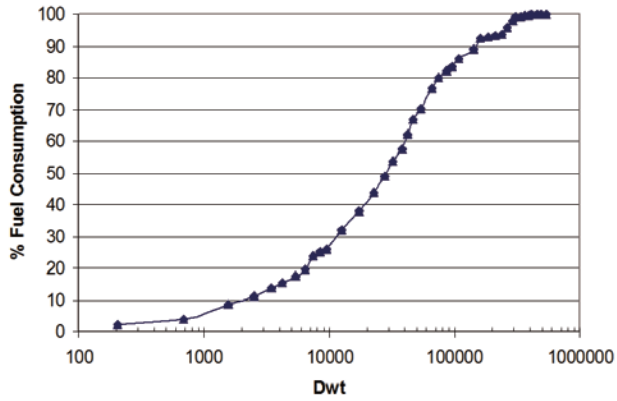

Figure 4. Modeled main engine fuel consumption as function of ship size in Dwt for the ocean-going cargo and passenger fleet above or equal 100 GT.

gives an estimate for total fuel consumption of 152 and 166 Mt for 1996 and 2000, respectively.

2.4. International Versus Domestic Bunker Consumption

[20] Operational data from Norway indicate that dry cargo ships between 500 and 3000 GT operate in domestic transport 80% of their time (Statistics Norway, 2000, http://www.ssb.no/emner/10/12/40/nos_sjofart/arkiv/nos_c582/nos_c582.pdf). Corresponding figures are valid for tankers between 100 and 3000 GT as well.

[21] The Norwegian International Ship register (NIS) is exclusively for ships in international trade, while the Norwegian Ordinary Register (NOR) includes ships mainly in domestic trade. In all, 96.4% of the NIS-registered fleet is larger than 1000 gross tons [*TheNorwegian Maritime Directorate*, 2000]. The *Norwegian Shipowner Association* [2000] (see http://www.rederi.no/infogroup.asp?infogroupID=2117) provides statistics for the Norwegian fleet in international trade with a breakdown on both NOR and NIS ships. By comparing the size distribution of the NOR fleet with the number and average size of the NOR ships sailing in international transport, we can conclude that ships below 2000–3000 gross tons typically operate in domestic transport.

[22] For nonpassenger vessels one may assume that one gross ton is about 1.5–2 Dwt [*Endresen and Sørgård*, 1999; *Norwegian Shipowner Association*, 2002] (see http://www.rederi.no/Article.asp?ArticleID=2848). Thus ships larger than 2000 gross tons, or about 3–4000 Dwt, are in international trade and smaller ships are in domestic trade. Figure 4 shows the modeled cumulative fuel consumption as a function of ship size. About 15% of the fuel consumption originates from ships less than 4000 Dwt and about 15% of the atmospheric emissions quantified through the model presented herein are related to domestic transport.

[23] The domestic bunker consumption (assumed to be 15% of total) is in the same range as the sum of the combined port consumption (assumed to be 5% of total) and auxiliary engine consumption during sailing (assumed to be 10% of total). Thus the total modeled fuel consumption of 132 Mt in 1996 and 144 Mt in 2000 for the main engine(s) seems to be a representative estimate of the total fuel consumption for the world fleet in international transport.

2.5. Comparison With Other Studies

[24] *Corbett and Fischbeck* [2000] use ship brake horsepower data and engine brake-specific fuel consumption data as basis to model ship emissions. The estimated fuel consumption of 170 Mt for the international commercial cargo fleet is 20% higher than our estimate. Some of the cargo-carrying ships above or equal 100 GT [*LR*, 1996] are in domestic trade and are therefore not part of the international bunker fuel inventory. Domestic marine fuel consumption is, however, significant and was 22 Mt (including inland waterways and coastal shipping, but excluding fishing vessels) for OECD countries in 1998. The corresponding sale to marine international transportation was about 84 Mt for these countries in 1999 [*International Energy Agency* (*IEA*), 2001].

[25] Recently, a study submitted by Japan to IMO [*Japan*, 2000], suggested that tankers, bulkers, and container vessels contributed 31, 30, and 32%, respectively, of the total fuel consumption (probably 140 Mt). The annual consumption is estimated separately for tankers, bulkers, and container vessels from the amount of cargo transported in ton-mile, and ship specific fuel consumption data. This distribution corresponds well with our distribution given in Table 5, except for container vessels.

2.6. Uncertainty

[26] The variability and uncertainty in estimates for ship emissions are discussed by *LR* [1995], *EMEP/CORINAIR* [1999], *Corbett et al.* [1999], *Skjølsvik et al.* [2000], and *EPA* [2000]. The uncertainty in each parameter of equation (1), including main assumptions, is addressed below with an estimate for the uncertainty in total fuel consumption and emissions. It is important to appreciate that the uncertainties in equation (1) arise as a result of the variability in the estimates for the individual ship classes. This variability can be assumed to be independent between vessel classes.

[27] The total engine power for each vessel class was estimated by exploiting the statistical relationship between Dwt and engine power. The uncertainty associated with this estimate was analyzed by comparing the estimated installed engine power with data from specific ships. Data for 3954 crude oil and ore bulk carriers (LRFairplay database, 2002) representing 52% of the world cargo fleet tonnage were analyzed and the deviation from our estimation was found to be ±11% for a given ship size class. In total, calculations based on statistical relationships gave 3% higher engine power estimates than using the specific fleet data. The engine power estimates for the crude oil and ore bulk carriers were 2 and 5% higher than specific data, respectively. This indicates that some of the variations cancel out in sum and reduce uncertainty in estimates for the entire fleet or ship types. Our model is probably biased and overestimates installed engine power with some 3–5%, with a corresponding overestimate in fuel consumption and emissions.

[28] The assumed engine type distribution for the specific vessel classes could potentially affect the fuel consumption. A separate test comparing estimates based on the model distribution with actual engine types indicates that this error source is small and can be ignored in the overall estimate.

[29] We have assumed that fuel consumed by auxiliaries account for 10% of main engine fuel consumption, and arguments in section 2.2 suggest that this is realistic. We expect that total fuel consumption by auxiliary engines is within 5–15% of the total main engine consumption during voyage. Thus the uncertainty in total fuel consumption is assumed to be on the order of ±5%.

[30] In-port emissions seem to range between 2 and 6% of the total emissions (see section 2.3) and are not included in our inventory. Thus our approach underestimates the total fuel consumption and emissions with about 4%. This effect will compensate for the overestimation related to the engine power estimates.

[31] A recent analysis of the operating profiles for 6712 individual vessels in The Automated Mutual-assistance Vessel Rescue system (AMVER) fleet (E. Carroll, personal communication, 2002) illustrates that there is a good correlation between the size of vessel and time in service. Our assumed average operating profiles agree well not only with these individual operational profiles, but also with profiles in the shipping movement database Seasearcher (Lloyd's Maritime Information Services, 2002, available as http://www.seasearcher.com) and average profiles reported for 453 very large crude oil carriers (VLCCs) tracked in 1991 by Clarkson (results given by *Wijnolst and Wergeland* [1997]). However, some variations between vessel types/sizes are observed and this has not been taken into account in this study. This types/sizes effect is also illustrated in a recent study submitted to IMO by United Kingdom, following 1580 cargo vessels [*United Kingdom*, 2002]. Based on the above data, we have judged the uncertainty in total fuel consumption and emissions to about ±10%.

[32] This paper applies an average engine load of 0.7 (see section 2.1), but engine service loads depend on vessel type and size, as well as on current bunker prices and freight rates. The average engine load profile varies between ships, as reported for 453 VLCCs tracked in 1991 by Clarkson (results given by *Wijnolst and Wergeland* [1997]). The reported average speed was 11 knots, but the variations were substantial, ranging from 10 to 13.6 knots. Moreover, operational data from Frontline's vessels illustrates that ballast voyages at the same speed use significantly less amount of bunker, compared with voyages in loaded conditions (Frontline Management, 2001, http://www.frontline.bm/fleetlist/index.php3). This is also supported by Wijnolst and Wergeland (Figure 8, p. 223). We expect that the uncertainty in total fuel consumption resulting from this parameter is on the order of ±10%.

[33] The assumed average specific fuel consumption may also introduce an error. Alternative average specific fuel consumption data evaluated by *Whall et al.* [2002] and *EPA* [2000] indicate an expected error of less than ±5%.

[34] The variability of emission amounts between ships is significant as illustrated by *LR* [1995], *Skjølsvik et al.* [2000], and *EPA* [2000]. We expect the uncertainty in the average NO_x emission factors to be about ±10%. The uncertainty in the average CO_2 emission factor is small and less than ±1%. These estimates are in line with those of *Skjølsvik et al.* [2000]. We expect the uncertainty in the average SO_x emission factors to be about ±10%, based on the average sulphur content for the most common marine fuels [*Cullen*, 1997]. The uncertainty in the average emission factor for the other compounds is probably higher and in the range ±10–30%.

[35] From the analysis presented above, we have estimated the uncertainty in total fuel consumption to be about ±16%, assuming that the overestimate in engine power balances the underestimate of in-port fuel consumption. Moreover, we have assumed that the uncertainty figures given above are independent and representative estimates for standard deviations. Calculated bunker fuel consumption is found to be in agreement with international sales statistics (see section 3). This indicates that our uncertainty estimate is reasonable. We may combine uncertainty in fuel consumption with uncertainty in emission factors to derive uncertainty in the emission inventories. It follows that the uncertainty in total CO_2 emissions corresponds to the uncertainty in fuel consumption, i.e., ±16%. The uncertainty in total SO_x and NO_x emissions is estimated to be about ±19%. The uncertainty for the other compounds is found to be within ±19–34%, assuming an uncertainty in average emission factors of ±10–30%.

3. International World Fleet Fuel Consumption

[36] Fuel consumption and the subsequent emissions by cargo and passenger vessels were discussed in section 2. In this part we will estimate and discuss the total international bunker sale and consumption by the world fleet. We will argue that the modeled international fuel consumption from cargo and passenger vessels above or equal to 100 GT is likely to be 132 and 144 Mt with reference to the years 1996 and 2000, respectively. *Skjølsvik et al.* [2000] estimated total fuel sales to ships in international trade during 1996 as 138 Mt, while IEA reported 147 Mt bunker fuel sold during year 2000 [*IEA*, 2003]. However, a fraction of the bunker sales includes consumption by noncargo and navy ships in international traffic. The amount consumed by these ships is discussed below.

3.1. Noncargo Vessels

[37] The noncargo fleet consists of about 40,000 vessels mainly operating in domestic waters, and represents only 5% of the total GT for the ocean-going fleet (Table 1). It can broadly be categorized into 25,000 fishing vessels and 15,000 service vessels (offshore, towing, pushing, and dredging) [*LR*, 2000]. The average size of these vessels is only about 700 GT compared to 11,000 GT for the cargo-carrying fleet (including passenger vessels). Most of the noncargo vessels have less operational hours (except for large offshore and fishing vessels) but more engine power for high-speed and service operations (offshore, towing etc.), compared with cargo-carrying vessels. The noncargo vessel international consumption may be estimated by subtracting the total international bunker sales from the modeled cargo-carrying consumption (including passenger vessels). The result would be obscured by the uncertainty of the bunker sales statistics. We evaluate a best estimate to be an international marine bunker sale of about 138 Mt for 1996 [*Skjølsvik et al.*, 2000] and 147 Mt for 2000 [*IEA*, 2003]. Our estimate for the cargo-carrying fleet (including passenger vessels) in international trade amounts to 132 Mt for the year 1996 and 144 Mt for the year 2000. Thus compared with the above sales statistics, the contribution

Table 6. Distribution of 1996 Fuel Consumption for Ship Categories Assumed to Contribute to the International Bunker Fuel Statistics[a]

	Cargo and Passenger Ships (Above or Equal to 100 GT)[b]	Other Ships (Above or Equal to 100 GT)[b]	Navy Ships (Above 100 t Displacement)	Sum
Normal cruising				
Main engine(s)	125–135	20–30		145–175
Auxiliary engine(s)	10–15	2–4		10–20
Port operations	5–8	2–3		5–10
Sum	140–160	25–35	4–5	170–200
Reported as				
International bunkers	125–135	5–10	1–3	130–150
National bunkers	15–25	20–25	1–3	35–50

[a]All Figures in Mt.
[b]According to the *LR* [1996] categorization.

from noncargo vessels operating internationally is likely to be approximately 5 Mt.

3.2. Navy Fleet

[38] The navy fleet consists of close to 20,000 vessels, including 750 submarines [*Adcock and Stitt*, 1995]. Only about 1300 vessels are larger that 100 t standard displacement (including 520 submarines of which 190 are nuclear powered) [*Calhoun*, 1999]. The larger vessels include 60 aircraft carriers/cruiser (typically above 10,000 t) and 750 destroyers/frigates (typically in the range 2000–10,000 t). Aircraft carriers are fewer, but are the largest navy vessels with displacement typical in the range of 80,000–100,000 t [*Calhoun*, 1999] (The Haze Gray and Underway database, 2001, available as http://www.hazegray.org/worldnav). An average size of the 1300 large navy vessels is estimated to be 5000 t displacement (on the order of 20,000 GT), while the average size of the cargo fleet is about 20,000 Dwt (10,000–15,000 GT). The navy vessels have less operational hours but more engine power for high speed, and an upper limit estimate is that these navy ships are in international trade and they account for a fuel consumption proportional to the number of vessels, i.e., about 3% (1300 navy vessels) of the ocean-going cargo and passenger fleet by number and bunker fuel consumption. Thus the contribution is small.

3.3. Fuel Consumption by the Cargo Versus the Noncargo Fleet

[39] The international fuel consumption by the noncargo fleet is relatively small compared to the cargo and passenger fleet. Table 6 shows a summary for 1996 of the fuel consumption by the ship categories assumed to be the main contributors to the international bunker fuel statistics. Our best 1996 estimate of international fuel consumption is 130–150 Mt (Table 6) and seems to be a representative estimate of the total fuel consumption for the world fleet in international transport subject to IMO regulations. Our estimated fuel consumption corresponds well with the sales numbers reported by *Skjølsvik et al.* [2000]. However, for 1996, *The Energy Statistics Yearbook* reported 123 million tons of oil equivalent (Mtoe) fuel supply to international transportation [*United Nations*, 1998] while IEA reported 130 Mtoe [*IEA*, 2003]. Year 2000 estimates should be 140–160 Mt, based on 147 Mtoe bunker reported sold in year 2000 [*IEA*, 2003]. The sales number reported by the Energy Information Administration (EIA) is not used in this study, according to recommendations by *Skjølsvik et al.* [2000].

[40] Our model provides a separation into national and international fuel consumption, and related emissions relevant for the regulatory regimes. The model result indicates that the total consumption for the entire fleet of about 106,000 vessels should amount to 170–200 Mt during 1996 (Table 6), which is considerably higher than estimates given by *Corbett et al.* [1999]. Corbett et al. estimate international bunker fuel usage for 1992 and 1993 to be 140 and 147 Mt, respectively. These estimates are valid for the entire fleet of 106,000 vessels, while only approximately 50% of these vessels (by number) are engaged in international transport.

4. Modeling of VOC Emissions From Crude Oil Transport

[41] This section presents a model for estimating VOC emissions during transport and cargo handling form the large ocean-going crude oil carrying fleet. The model enables an independent approach to quantify fuel consumption for a fleet segment by means of trade data.

4.1. VOC Emission Model Description

[42] A separate model has been developed to quantify VOC emissions from crude oil carriers greater than 50,000 Dwt. A Geographical Information System (GIS) is used to simulate the global crude oil flow in 1996. The GIS model is based on separate calculations of emissions in loading ports, on trade, and at unloading ports, according to the transported amount of crude oil per year for a specified sea route. The majority of crude oil transportation is assumed to be done by three tanker types: Aframax, Suezmax, and VLCC with an assumed average size of 75,000, 150,000, and 250,000 Dwt, respectively. The crude oil volumes transported by these tanker types and associated trade routes are taken from the work of *Fearnleys* [1997], the EIA (see World Petroleum Supply and Distribution, 2001, http://tonto.eia.doe.gov/FTPROOT/international/021999. pdf and Fact Sheet for South China Sea Region, South China Sea Tables and Maps, http://www.eia.doe.gov/cabs/schinatab.html), *United Nations* [1998], and AMVER (E. Carroll, personal communication, 2001). Twenty-nine main crude oil routes are identified, comprising 88% of the 1466 Mt crude oil transported during 1996 (combined carriers ar not included) [*Fearnleys*, 1997].

Table 7. Emission Factor Crude Oil Losses During Loading, Transport, and Unloading[a]

Mode	Emission Factor	Unit
Loading	0.1%	of loaded weight
Transport	150	mg/week l
Unloading	129	mg/l

[a]From *EPA* [1995], *Endresen et al.* [1999], *EMEP/CORINAIR* [1999].

The number of days in open sea is calculated using the distance table in Lloyd's Maritime Atlas [*LR*, 1999a, 1999b], assuming an average speed of 15 knots. An estimate for the number of voyages on each route and the related number of tank operations (loading, unloading) is thus found. The amount and location of the VOC emissions can be quantified by means of VOC emission factors for crude oil during loading, transport, and unloading. Exhaust gas emissions related to this transport are estimated using fuel consumption data in cruise and port mode [*EPA*, 2000; Frontline Management, 2001, http://www.frontline.bm/fleetlist/index.php3).

[43] The geographical locations for the emissions are modeled by defining 85 polygons (port areas and ship lanes). The lane width of the trade routes is assumed to be 200 km, in accordance with observed patterns for crude oil traffic (E. Carroll, personal communication, 2001). The emissions within each polygon are then mapped to a $1^\circ \times 1^\circ$ grid. Emission factors are given in Tables 4 and 7. Unloading and transport factors are based on AP-42 emission factors [*EPA*, 1995] (see http://www.epa.gov/ttn/chief/ap42/ch05/final/c05s02.pdf). The loading factor is based on a review of hydrocarbon emission data [*Endresen et al.*, 1999] (available as http://research.dnv.com/marmil) and factors presented by *EMEP/CORINAIR* [1999]. The VOC distribution (Figure 3) is based on separate emission calculations for each defined port-polygon and sea-route polygon, before transforming the VOC emission into grid cells. The global distribution of VOC emissions in ports and the main sea routes is integrated in the inventories as an individual gas component.

4.2. VOC Emission and Bunker Consumption

[44] The modeled VOC emissions during transport and cargo handling of 1300 Mt crude oil is estimated to be close to 2 Mt, and corresponds well with estimates given by *Martens* [1993]. The VOC emissions are distributed as 70% during loading, 27% at voyage, and 3% during unloading. Emission reduction using technology improvements is not taken into account. The fuel consumption for the transport of the 1300 Mt crude oil was estimated to be 16.8 Mt (covering 88% of the crude oil transport). The alternative statistical model calculates an annual fuel consumption of 20.2 Mt for tankers above 50,000 Dwt. The agreement is good when taking into account that 16.8 Mt bunker fuel reflects 88% of the annual crude oil transportation.

5. Geographical Distribution of Emissions

[45] The global emission inventories are distributed geographically according to global vessel traffic data in this section.

5.1. Distribution Methods and Global Traffic Data

[46] The modeled atmospheric emissions may be distributed geographically according to the ship reporting frequency and ship size by using the following equation:

$$M_{g,j} = \frac{M_g S_j}{S} = M_g I_j, \tag{3}$$

where

$M_{g,j}$ emissions for the individual exhaust gas component g in geographical cell j, kg pollution;
M_g total emissions for the individual exhaust gas component g (Table 5), kg pollution;
S total number of ship observations or total accumulated GT of ships reporting;
S_j number of ship observations or accumulated GT in cell j of ships reporting;
I_j emission indicator in cell j, referring to relative reporting frequency or relative reporting frequency weighted by the ship size (given by GT).

[47] The modeled atmospheric emissions M_g is based on equation (1) and given in Table 5. The impact modeling is based on these emission data, including the auxiliary emissions. The emission indicator, I_j, is based on global ship reporting frequencies collected by The Comprehensive Ocean-Atmosphere Data Set (S. J. Worley, personal communication, 2001), PurpleFinder (G. Whitby-Smith, personal communication, 2001), and AMVER (E. Carroll, personal communication, 2001). The reporting frequency weighted by the ship size is only available from the AMVER data. A description of each data set is given below.

5.2. Description of the COADS Distribution

[48] COADS from the National Centre for Atmospheric Research (NCAR) and the National Oceanic and Atmosphere Administration (NOAA) are the most extensive collection of surface marine data available. The main source of marine surface observations for COADS is the Voluntary Observing Ships (VOS) fleet [*Worley*, 2001] with the objective to obtain a best possible coverage of meteorological observations over the sea. The ship location data are based on reporting of routine meteorological observations, ideally at 6-hour intervals according to procedures by the World Meteorological Organization (WMO). The total VOS-fleet includes about 7000 vessels, and can broadly be categorized into 1800 (26%) cargo and passenger vessels, 1000 research, support, and fishing vessels, and 4200 vessels not specified (see http://www.wmo.ch/web/ddbs/publicat.html). In 1996, a total of 1,347,637 marine reports were registered, indicating that only about 1000 ships are reporting four times a day and that most ships report infrequently. For this study, we used the COADS standard version including only surface marine reports from ships statistically summarized on a monthly basis with a $1^\circ \times 1^\circ$ spatial resolution (S. J. Worley, personal communication, 2001).

5.3. Description of the Purple Finder Distribution

[49] Pole Star Space Applications Limited has developed PurpleFinder®, a Web-based interface that can be used to "locate, communicate with and monitor fixed or mobile assets on a global scale" (available as http://

Table 8. Relative Distribution of Emission Indicator at the Main Oceans[a]

	COADS				PF				AMVER				AMVER (GT)			
Latitude	Atl Sea	Pac Sea	Ind Sea	Med Sea	Atl Sea	Pac Sea	Ind Sea	Med Sea	Atl Sea	Pac Sea	Ind Sea	Med Sea	Atl Sea	Pac Sea	Ind Sea	Med Sea
60°–90°N	6.0	0.1			1.1	0.0			0.3	0.0			0.2	0.0		
40°–60°N	25.3	9.3		1.0	14.3	1.9		3.9	9.1	7.1		0.7	7.6	6.3		0.6
20°–40°N	12.3	10.8	0.9	3.4	11.0	10.7	6.6	7.1	16.9	13.7	2.3	3.6	14.5	12.8	3.7	3.9
0°–20°N	6.0	6.3	4.4		9.0	12.0	6.8		9.8	9.8	7.7		10.2	9.7	10.4	
0°–20°S	1.9	2.7	1.7		2.4	3.0	2.3		3.3	3.6	2.7		4.1	2.8	3.3	
20°–40°S	2.0	2.8	2.0		3.1	1.8	2.5		3.0	2.4	3.5		3.6	1.6	4.4	
40°–90°S	0.6	0.5	0.2		0.1	0.3	0.0		0.2	0.4	0.0		0.2	0.3	0.0	
90°N–90°S	54.0	32.5	9.2	4.4	41.0	29.8	18.2	11.0	42.6	36.8	16.3	4.3	40.3	33.5	21.7	4.5

[a]The indicator is given by the reporting frequency for all data sets, and in addition by GT for AMVER (GT). Atl, Atlantic; Pac, Pacific; Ind, Indian; and Med, Mediterranean.

www.purplefinder.com). PurpleFinder (PF) communicates with each vessel's Inmarsat-C terminal and automatically reports position. Statistical analysis of ship locations and trade routes may be compiled from the position reports. For this study, PF has supported us with a fleet data with a $1° \times 1°$ spatial resolution for year 2000 that contains 685,492 vessel observations for 1863 ocean-going cargo vessels (excluding Fishing, Coastguard, and Navy vessels) [*PF*, 2001].

5.4. Description of the AMVER Distribution

[50] The AMVER system is used to track participating merchant vessels at sea. These ships submit information including position to the AMVER database (see U.S. Coast Guard, 2003, http://www.amver.com). Participation in AMVER is generally limited to merchant ships of all flags above 1000 GT, on a voyage of 24 hours or longer (see AMVER, 2001, http://www.amver.com). In this study, the calculated average size is about 40,000 GT, illustrating that AMVER represents very well the international cargo fleet. There are currently 12,550 vessels from more than 100 nations in the AMVER database, with approximately 2700–3000 vessels reporting mainly daily (E. Carroll, personal communication, 2001). In the AMVER system, more than 100,000 voyages are tracked each year (see AMVER, 2001, http://www.amver.com). The advantage with the AMVER data set is that ship type and size can be identified. Consequently, the atmospheric emissions can be distributed accordingly and not only by total amounts according to reporting frequency as for COADS and PF. The year 2001 AMVER data set was not complete (missing 120 days). The applied AMVER data (with a $1° \times 1°$ spatial resolution) cover 300 days and include some data for year 2000 to extend the database (E. Carroll, personal communication, 2001). There is some overlap between the COADS and AMVER data sets (J. Hessenauer, personal communication, 2001), and about 33% of the AMVER vessels are weather observation vessels (D. Horton, personal communication, 2003).

5.5. Evaluation of the Distributions

[51] In this study, we have used the monthly summary data from COADS for the year 1996 to distribute the modeled exhaust gas emissions. The global traffic density based on COADS is shown in Figure 1. Moreover, we have developed two alternative distributions, one based on AMVER and the other on PF. The reference year for these data is 2000, but should be representative for year 1996 as well. The AMVER distribution is shown in Figure 2. The distribution of the emission indicator, I_j, for PF, COADS, and AMVER is presented in Table 8.

[52] Figures 5 and 6show that the regional distributions of the emission indicators for AMVER and PF to a large degree correspond to, but they are significantly different from COADS. Some of the deviation may be explained by the fact that AMVER and PF mainly represent the international cargo fleet, while COADS includes a large fraction of noncargo vessel (Table 9), mainly in national traffic. Table 9 illustrates that the AMVER fleet best reflects the international cargo fleet by vessel types, size, and reporting frequency, followed by PF. The AMVER database enables

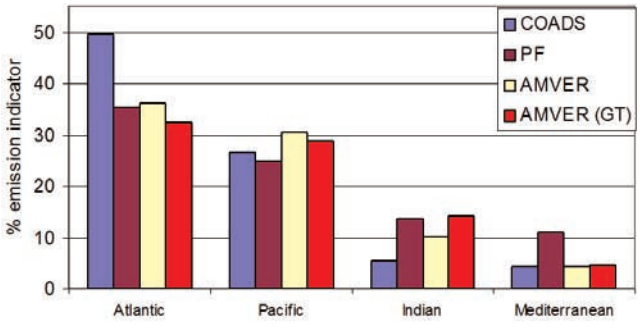

Figure 5. Relative distribution of emission indicator at the main oceans for the Northern Hemisphere. The indicator is given by the reporting frequency for all data sets, and in addition by GT for AMVER (GT).

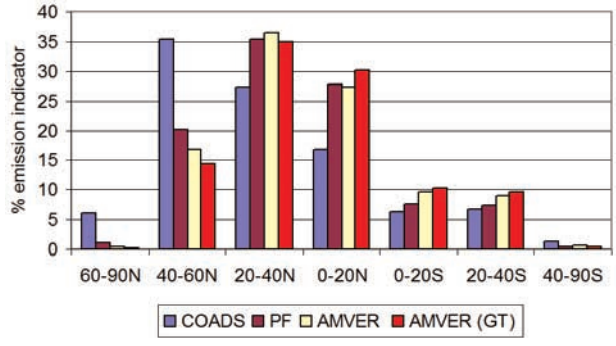

Figure 6. Relative distribution of emission indicator at different latitudes. The indicator is given by the reporting frequency for all data sets, and in addition by GT for AMVER (GT).

Table 9. Comparison of the Data Sources

Source	Number of Vessels	% Cargo Ships	Average Daily Plot	Average GT	Reference
COADS	6931[a]	20–50	3500	17,000[b]	WMO[c], *COADS* [2001]
PF	1863	>90	2000	35,000[d]	*PF* [2001, 2002]
AMVER[e]	12,550[a]	>90	2900	40,000	*AMVER* [2001a, 2001b]

[a]Not every vessel is reporting daily.
[b]Estimated from the average length of about 2000 VOS-vessels.
[c]See http://www.wmo.ch/web/ddbs/publicat.html.
[d]Estimated from a average size of 75–80,000 Dwt [*PF*, 2002].
[e]Participation in AMVER is generally limited to merchant ships of all flags over 1000 GT, on a voyage of 24 hours or longer (see AMVER, 2001, http://www.amver.com).

identification of ship type and size for about 85% of the observations. However, AMVER seems to slightly overrepresent large cargo vessels (Figure 7) and the dry bulk cargo category (Figure 8), likely because participation in AMVER is generally limited to merchant ships of all flags over 1000 GT, on a voyage of 24 hours or longer (J. Hessenauer, personal communication, 2001). The largest absolute deviation between emission indicator based on reporting frequency and weighted reporting frequency (AMVER) is in the Indian Ocean (5.4%). This is a result of the dominating crude oil transport in this area. Our best estimate based on the above discussion is that 80% of the traffic is in the Northern Hemisphere, and distributed with 32% in the Atlantic, 29% in the Pacific, 14% in the Indian, and 5% in the Mediterranean Oceans. The remaining 20% of the traffic in the Southern Hemisphere is approximately equally distributed between the Atlantic, the Pacific, and the Indian Oceans (Table 8).

[53] Considering the number and types of vessel reporting, typical vessel size, and reference year, we prefer the AMVER data set for distribution of emissions from international traffic. We recommend the AMVER data set. The relative reporting frequency weighted by the ship size may be applied to take into account large variation in emission between small and large vessels.

5.6. Comparison With Other Studies

[54] COADS was used by *Corbett et al.* [1999] to quantify global inventories of nitrogen and sulphur emissions from international maritime transport. According to their calculation, more than 50% of the exhaust gas emissions take place in the North Atlantic (between North America and Europe). However, PF and AMVER data indicate that about 35% of the international traffic is in this region (Table 8 and Figures 5 and 6). It is not possible from port data [*ISL*, 1997] summarized regionally by *Worley* [1999] and bunker sales statistics [*United Nations*, 1998] by region (Table 10) to conclude that half of the traffic takes place in the North Atlantic. For example, Asia accounted for 57% of the 1.5 million ship arrivals in 1996, covering regional traffic as well as international traffic. COADS will probably result in too high emissions in the northern Atlantic and in particular between 40° and 60°N (Figures 5 and 6), likely caused by overrepresentation of noncargo vessel records (mainly research, support, and fishing vessels). In addition, COADS data seem to include some stationary "vessels" (oil rigs) for the North Sea area [*Worley*, 2002], and for regional studies covering the areas with stationary vessels, the error may be significant.

[55] For the year 2000, *Whall et al.* [2002] estimated the total emissions from shipping movements in the EMEP domain. The EMEP area is defined in polar conical projection and is approximately the area east of 40°W, west of 60°E, and north of 30° [*Whall et al.*, 2002]. The international vessel emissions were estimated to be in the range 35–40% of the total in this study. The total CO_2 emissions were estimated to be 153 Mt for vessels and ferries, and the related international part is then about 57 Mt. The total SO_2

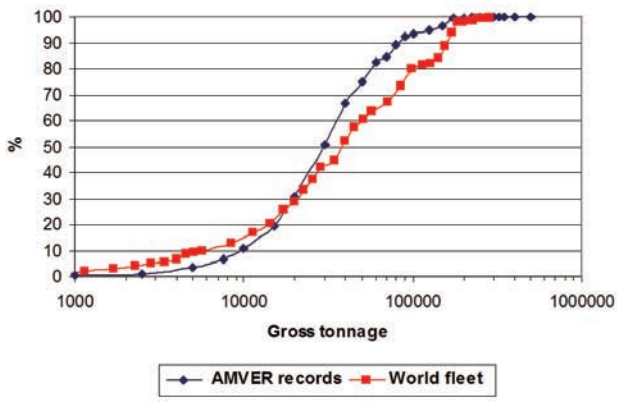

Figure 7. Comparison between tonnage distribution of observed ship-specific AMVER records and of vessel in the cargo and passenger fleet assuming that one GT is 1.8 Dwt (based on data from 4500 DNV classed vessels).

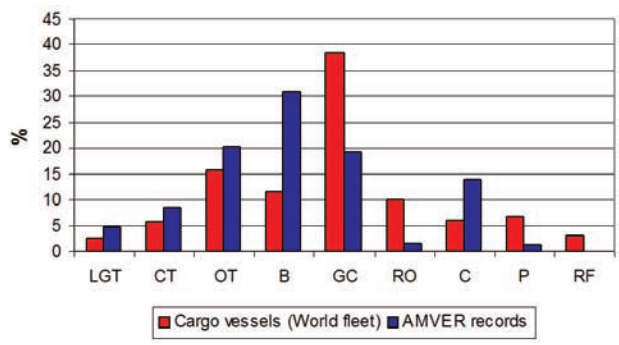

Figure 8. Comparison between distribution of vessel in the world fleet and distribution of observed ship-specific AMVER records (LGT, liquid gas tanker; CT, chemical tanker; OT, oil tanker; B, bulk; GC, general cargo; RO, RO-RO cargo; C, container; P, passenger cargo; and RC, refrigerated cargo).

Table 10. Comparison Between Port of Calls and International Bunker Sales for 1996

Region	Port of Calls,[a] %	Bunker Sales,[b] %
Africa	3.9	4.3
America	7.2	18.1[c]
Asia	56.9	38.4
Europe	30.5	37.8
Oceania	1.5	1.4

[a]Data from *ISL* [1997] summarized by *Worley* [1999], covering 80 countries and more than 250 ports.
[b]*United Nations* [1998].
[c]*United Nations* [1998], but USA sales number is based on data from Foreign Trade Division of the U.S. Department of Commerce's Bureau of the Census [*EPA*, 1999] (see http://yosemite.epa.gov/oar/globalwarming.nsf/UniqueKeyLookup/SHSU5BMQ5D/$File/1999-inventory.pdf), according to recommendations by *Skjølsvik et al.* [2000].

emissions were estimated to 2.5 Mt, and thus the related international fraction is approximately 0.9 Mt. The sulphur content assumed for residual fuel in this study was 2.7%. For the same area (EMEP), using AMVER data and our emissions inventory (Table 5), the CO_2 emissions are estimated to be 55 Mt and the SO_2 emission is 0.8 Mt (year 2000). Lloyd's have made emission inventories with reference to year 1990 for the main areas in the EMEP area, not including CO_2 emissions [*LR*, 1995, 1998, 1999a, 1999b]. Lloyd's estimated the SO_2 emissions of 2.8 Mt within the EMEP area (given by *Jonson et al.* [2000a, 2000b]). The sulphur content assumed for heavy fuel in these studies was 2.7%. Assuming that the international fraction is 35–40% (as above), the SO_2 emissions from ships in international trade are estimated to be about 1.1 Mt. For the same area, our 1996 estimates indicate some 0.7 Mt SO_2 using AMVER data and emissions inventory (Table 5).

[56] *Streets et al.* [2000] estimated the international SO_2 emissions in the Asia waters to be 0.817 Mt in 1995, based on oil, bulk, and miscellaneous cargo transported with average characteristic vessels, also including in-port emissions (2.2% of the total emissions). The sulphur content assumed in this study was 3%. SO_2 emissions in 1996 may be estimated to 0.9 Mt, assuming a growth rate of 5.9% reported by Streets et al. In 1996, our work estimated about 1.1 Mt of SO_2 emitted in this area when using a lower sulphur content (Table 4) and including emissions from passenger vessels.

[57] These emission inventory comparisons indicate some deviations that may be explained by use of different reference year, calculation methodologies, emission factors (average sulphur content, etc.) and fleet segments covered. Notably, there is good agreement between our ship emission inventories and inventories developed by *Whall et al.* [2002] for the EMEP area.

6. Global Modeling of the Effect of Ship Emissions

[58] Several model experiments are run with the Oslo CTM2 using the global emission inventories compiled in sections 4 and 5, in addition to standard surface and atmospheric emissions, as described further down. First, a description of the CTM is given followed by a description of the basic ozone chemistry. The ozone, CO, and NO_x climatologies including the AMVER CO and NO_x emission data, are described in section 6.3. The relative importance of ship emission is then evaluated, first by comparing the AMVER run to one without ship emissions. Then some experiments with the other emission distributions (PF, COADS) and the AMVER emission data also including VOC and methane emissions are described. Finally, the radiative forcing from the CO_2, CH_4, ozone, and sulfate perturbations is estimated.

6.1. Model Description

[59] The Oslo CTM2 used to study the effect of ship emissions on atmospheric chemical composition is run in a T21 ($5.6^\circ \times 5.6^\circ$) resolution with 19 vertical levels from the surface to 10 hPa (a vertical resolution of approximately 1 km in the troposphere). The Oslo CTM2 uses off-line precalculated meteorological and physical data from the European Centre of Medium Range Weather Forecasts (ECMWF). The transport data are compiled for 1996 and monthly averaged results are presented. The model is run with 1-month spin-up to allow for the chemical tracers to adjust to the chemical environment and the last 12 months are used to describe the climatology. Transport is done using the second-order moment scheme [*Prather*, 1986]. Convection is based on mass flux data from the ECMWF convective parameterization [*Tiedtke*, 1989] and is done based on the surplus or deficit of mass in a column. Three-dimensional rainfall is used to estimate the wet removal of hygroscopic tracers, both for large-scale removal and in convective events. The chemistry scheme is a comprehensive scheme for chemically active compounds in the oxygen, hydrogen, nitrogen, and carbon families. The quasi steady state approximation integrator [*Hesstvedt et al.*, 1978; *Berntsen and Isaksen*, 1997] is used to solve chemical equations. Sulfur oxidation is done interactively with the oxidant chemistry. Photo-dissociation is done on-line using the Fast-J code with eight streams and rescattering of the radiation [*Wild et al.*, 2000]. Boundary layer turbulence is estimated using the Holtslag K-profile boundary layer scheme [*Holtslag et al.*, 1990].

[60] Surface emissions are primarily taken from the EDGAR database for anthropogenic emissions [*Olivier et al.*, 1996] while Muller data are used for natural emissions [*Müller*, 1992]. A complete reference to the emissions of primary compounds is given in Table 11. The lightning activity and thereby the NO_x production [*Price et al.*, 1997a] are distributed to be consistent with the convective activity in the model. NO_x emission from air traffic is based on the NASA-92 inventory. The ship emissions used are taken from the AMVER data including CO, SO_2, and NO_x only (Table 12). An additional perturbation run is performed with VOC and methane emissions (Table 13). Natural emission over ocean of DMS (CH_3SCH_3) from algae is included since about 90% of DMS is oxidized to SO_2. The annual and global-averaged emission data used are given in Table 14.

6.2. Chemical Processes Determining the Net Ozone Production in the Troposphere

[61] Ozone is a secondary chemical compound. Its formation and distribution are determined by the emission of

Table 11. Categories for Surface Emissions in the OsloCTM2 Model Together With Information About Their Temporal Variation and for Emission Values and Grid[a]

Categories	Values	Grid
Anthropogenic CO, NO_x, NMVOC, SO_2; no seasonal variation; in average, 12 different categories	Edgar 2.0: *Olivier et al.* [1996]	Edgar 2.0: *Olivier et al.* [1996], GEIA85: *Benkovitz et al.* [1996]
Soil (monthly averages) CO and NO_x	*Müller* [1992] (scaled down)	*Müller* [1992]
Vegetation (monthly averages)		
Acetone	*Singh et al.* [1994]	*Müller* [1992]
Aromatics	*Müller* [1992]	*Müller* [1992]
Hydrocarbons	Mozart: *Brasseur et al.* [1998], *Hough* [1991]	*Müller* [1992]
Ocean (monthly averages)		
CO	*Müller* [1992] (scaled down)	*Müller* [1992]
Hydrocarbons	*Plass-Dulmer et al.* [1993] (scaled up a factor 2)	*Müller* [1992] (CO-grid)
DMS	*Kettle et al.* [1999]	*Kettle et al.* [1999]
Forest burning (monthly averages)		
Acetone	*Singh et al.* [1994]	*Müller* [1992]
Others (CO, NO_x, NMVOC)	Edgar 2.0: *Olivier et al.* [1996] (values up with factor 1/6 to include fires outside the tropics)	*Müller* [1992]
Volcanoes (SO_2)	*Graf et al.* [1997]	*Spiro et al.* [1992]
Lightning (NO_x)	*Price* [1997a, 1997b]	*Price* [1997a, 1997b]
Savanna burning (monthly averages)		
Acetone	*Singh et al.* [1994]	*Müller* [1992]
Others (CO, NO_x, NMVOC)	Edgar 2.0: *Olivier et al.* [1996]	*Müller* [1992]
Agricultural waste burning (monthly averages)		
Acetone	*Singh et al.* [1994]	Edgar 2.0: *Olivier et al.* [1996]/*Müller* [1992]
Others (CO, NO_x, NMVOC)	Edgar 2.0: *Olivier et al.* [1996]	Edgar 2.0: *Olivier et al.* [1996]/*Müller* [1992]

[a]Anthropogenic emissions are from the EDGARv2.0 Database [*Olivier et al.*, 1996] and for sulfur *Benkovitz et al.* [1996] for 1985 scaled to 1996 values. Natural emission distributions are from *Müller* [1992]. *IPCC Third Assessment Report* [2001], *Brasseur et al.* [1998, Mozart] and *Plass-Dulmer et al.* [1993] are used to scale some of the natural emissions in correspondence with more recently developed estimates for total emissions. For DMS emissions, the DMS concentrations in the ocean are from from *Kettle et al.* [1999] and flux parameterization from *Liss and Merlivat* [1986] with wind fields from the model. NO_x from lightning is from *Price* [1997a, 1997b].

primary pollutants like NO_x, CO, CH_4, and nonmethane hydrocarbons. Ozone formation occurs via the following sequence of reactions:

$$\text{(R1)} \qquad NO + HO_2 \rightarrow NO_2 + OH$$

$$\text{(R2)} \qquad NO_2 + h\nu \rightarrow NO + O$$

$$\text{(R3)} \qquad O + O_2 + M \rightarrow O_3 + M.$$

Carbon monoxide oxidation proceeds via the following reactions:

$$\text{(R4)} \qquad CO + OH \rightarrow CO_2 + H$$

$$\text{(R5)} \qquad H + O_2 + M \rightarrow HO_2 + M.$$

The significance of this reaction is to regenerate HO_2, which then participates in reaction (R1) to form OH and produces ozone through reactions (R2) and (R3).

[62] Methane is mainly lost in the atmosphere in the reaction with OH:

$$\text{(R6)} \qquad CH_4 + OH \rightarrow CH_3 + H_2O.$$

Further oxidation will lead to ozone formation in a similar way as in the sequence of reactions (R1)–(R3).

[63] The chemistry of ozone, methane, NO_x, and CO is therefore closely linked together through the above reactions.

[64] Although the abundance of NO_x is crucial for ozone formation in the atmosphere (reactions (R1)–(R3)), the number of ozone molecules formed is determined by the amount of CO and methane present.

Table 12. Yearly Total Emissions From Ship Engines Used for the Simulations Done With the OsloCTM2 Model[a]

Component	1996 (COADS)	2000 (PF, AMVER)
NO_x	3.29 (N)	3.63 (N)
CO	0.44 (C)	0.48 (C)
SO_2	3.01 (S)	3.41 (S)
CH_4		0.046
Hexanes and higher alkanes as hexanes		0.122
Ethene		0.072
Propenes + butenes + hexenes as propene		0.086
Aromatics as *m*-xylene		0.079

[a]Emissions are in Tg/yr; element is in parentheses after value when applicable. The methane and VOC emissions were only used in the simulations with the AMVER distribution. The individual VOC composition is from *Cooper et al.* [1996].

Table 13. Yearly Total Hydrocarbon Emissions From Crude Oil Transport (Evaporation During Loading, Transport, and Unloading) Used for the Simulation Done With the OsloCTM2 Model[a]

Component	2000 (AMVER), Tg
CH_4	0.294
Ethane	0.082
Propane	0.331
Butanes + pentanes as butanes	0.337
Hexanes + unidentified as hexanes	0.857
Aromatics as *m*-xylene	0.059
Total	1.959

[a]For the individual VOC composition the United States Enviornmental Protection Agency data on evaporation from crude oil tanks was used [*EPA*, 2002] (available as http://www.epa.gov/ttn/chief/software/speciate/index.html).

Table 14. Total Surface Emissions in OsloCTM2 for Different Chemical Components[a]

Components	Emissions
CO	1231.8
NO_x	39.39 (N) (+5 N from lightning)
Methane	467.9
Isoprene	220.0
Ethane	9.49
Propane	9.49
Butanes + pentanes as butane	40.55
Hexanes as hexane	29.23
Ethene	16.79
Propene + other alkenes as propene	15.09
Aromatics as *m*-xylene	74.81
Formaldehyde	1.99
Other aldehydes	4.94
Acetone	23.84
SO_2 (includes H_2S, all converted to SO_2)	82.31 (S)
DMS	11.96 (S)

[a]Emissions are in Tg/yr. Element is in parentheses after value, when applicable.

[65] A key factor in limiting the ozone formation in the atmosphere is the efficiency of NO_x removal from the atmosphere. Several reactions participate in the removal from the atmosphere, but in areas where NO_x is abundant it is lost through the following reaction with OH:

$$\text{(R7)} \qquad NO_2 + OH + M \rightarrow HNO_3 + M$$

followed by heterogeneous removal of HNO_3 by dry or wet deposition. Lifetime of NO_x in the troposphere is on the order of hours to days. The short lifetime in the troposphere means that there are large spatial and temporal variations in the NO_x distribution. This is essential for the estimates of net ozone production and change ozone distribution resulting from ocean-going vessels. Although the above reactions are the main reactions in the ozone-forming process, a large number of other reactions are involved in tropospheric ozone chemistry.

[66] As a result of the interaction of the above reactions, ozone formation in the troposphere is highly nonlinear as shown by *Isaksen et al.* [1978]. Although the efficiency of ozone formation to some extent depends on the emissions of other pollutants, the nonlinearity is strongly linked to the distribution of NO_x sources. Ozone formation becomes less efficient per NO_x molecule emitted at high NO_x levels. For instance, emissions of NO_x from ship over remote ocean areas, where background levels of NO_x in general are low, due to the absence of sources, can be very efficient in ozone formation.

[67] Although the above reactions are the main reactions in tropospheric ozone chemistry, a large number of reactions involving other compounds are affecting the oxidation process in the troposphere. These reactions are represented in the chemical scheme in the Oslo CTM2.

6.3. Description of Tracer Distributions

[68] The AMVER emission distribution is used in the perturbation studies since it is considered as the most realistic. The emission data are interpolated from a $1° \times 1°$ grid to the T21 (5.625°) resolution used in the CTM, and emissions are updated each month. All ship emissions are assumed to take place in the first model layer.

[69] Surface ozone, CO, and NO_x distribution for January and July are shown in Figures 9a and 9b, the somewhat high wintertime NO_x can partly be explained by small boundary layer mixing in the transport data. Since CO and NO_x are primary compounds and ozone is produced in the atmosphere through reactions involving NO_x and CO, the distributions of these compounds reflect the major source regions of CO and NO_x. Enhanced concentrations are found over industrial regions in the Northern Hemisphere. NO_x shows particularly large gradients in the distribution due to its very short chemical lifetime. The large variations in concentrations demonstrate that there are significant differences in the chemical activity in different regions, depending on the level of emission of pollutants. This is important since we want to estimate the impact of ship emissions in oceanic regions where pollution levels are low (part of the Atlantic Ocean) and oceans where the pollution levels are high (Norwegian Sea). In general, emission of pollutants is more efficient in producing ozone in low-polluted background regions than emissions in more polluted regions. Thus the emission inventories have to be accurate to simulate a reasonable ozone distribution and seasonal variation.

6.4. Ozone and NO_x Perturbation From Ship Emissions Using AMVER

[70] The perturbations in NO_x and ozone from ship emissions are obtained from two model runs: One basic run without ship emissions and one additional run where emissions from ship are included. The resulting perturbations in NO_x and ozone are shown in Figures 10a and 10b, respectively. The AMVER emissions have no seasonal variations, while the COADS data include a monthly variation in the emission. The effect of this variability is small, however, and insignificant compared to the uncertainty connected to the adopted sailing tracks. We therefore believe that neglecting seasonal variations in the AMVER emissions do not introduce significant uncertainties in the distribution and impact. The results demonstrate the importance of the nonlinearity in ozone formation. Over the North Sea where background NO_x levels are high, ozone formation is less efficient than in, for instance, over the Atlantic Ocean where background levels are low.

[71] Since the NO_x lifetime is short, the perturbation will closely follow the ship tracks as seen in Figure 10a. The largest effect is seen in January in the English Channel and North Sea, where there is an increase of about 500 ppt. A somewhat smaller effect is seen in the Mediterranean and off the coast of USA and over Indonesia, with an increase of around 200 ppt. In July the NO_x increase is pronounced over the Atlantic and Pacific but with lower maximum values. The variation is indicative not only of the seasonal variations in the NO_x emissions but also of the chemical activity. High chemical activities at northern latitudes in the summer season will cycle more NO_x and reduce the lifetime of NO_x. Part of the NO_x is stored as PAN in winter, thus there will be an extra loss of NO_x through dry deposition of PAN, and in addition, there is a larger heterogeneous loss of NO_x in winter through N_2O_5 and HNO_3. Thus we will have a higher NO_x increase in summer since the loss is smaller while the emissions are the same in January and July.

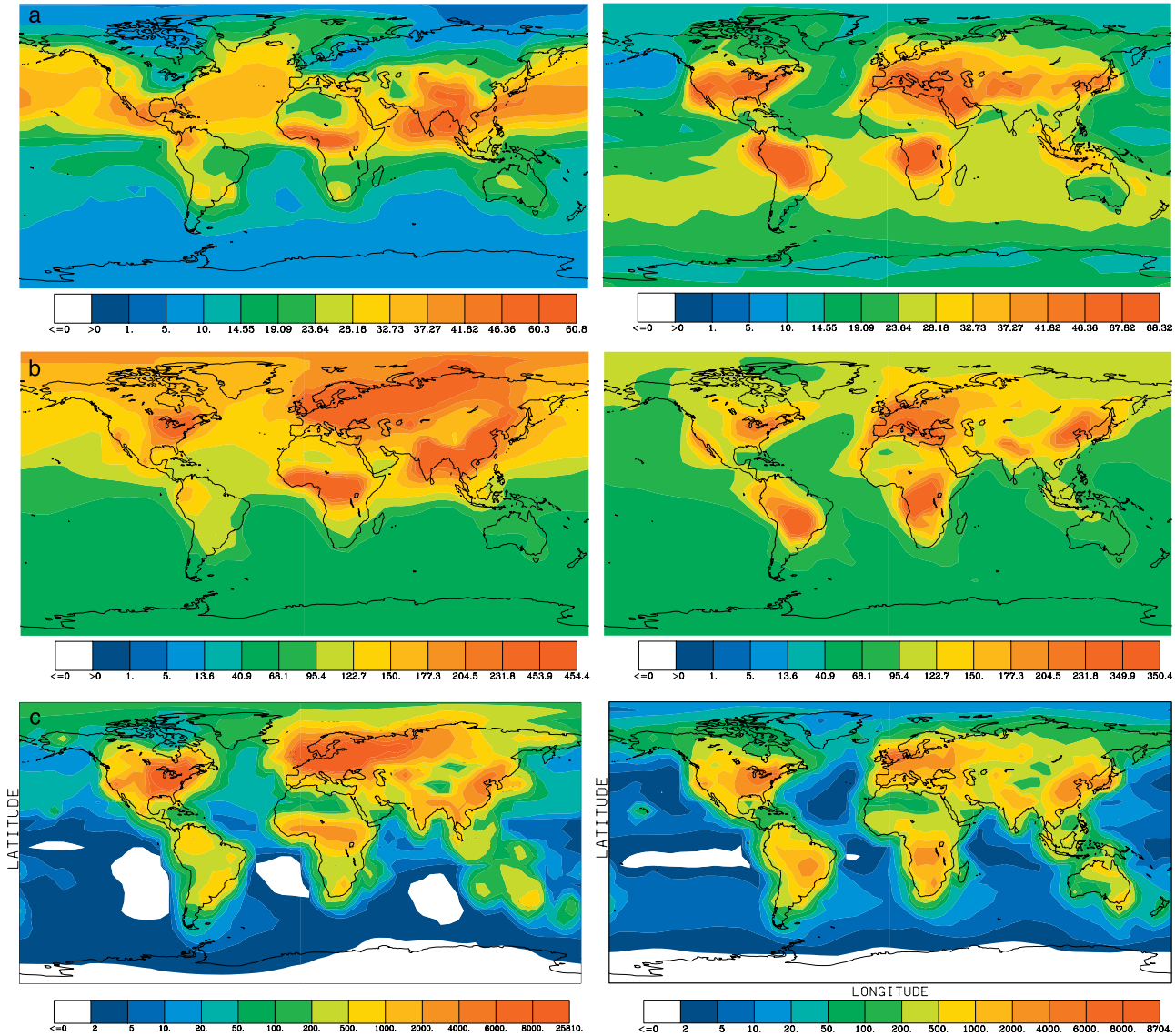

Figure 9. Monthly mean (a) ozone (ppb), (b) CO (ppb), and (c) NO_x (ppt) for January (left) and July (right) in the first model layer.

[72] Comparisons of modeled NO_y and NO_x with observations in oceanic regions affected by ship emissions have been done by *Kasibhatla et al.* [2000] and *Davis et al.* [2001]. In the North Atlantic the CTM2 seems to correspond better to observations than the values modeled by Kasibhatla et al. The CTM2 values are similar to the observed values for NO_y. For NO_x however, CTM2 overestimates the observations but significantly less than Kasibhatla et al. (see Table 15). In the North Pacific the overestimation of NO_x by CTM2 is of the same magnitude as found by Davis et al. In another study done by *Lawrence and Crutzen* [1999] the effects of ship emissions on the NO_x distributions inside and close to the major shipping lines are even larger. This is probably due to the narrower distribution of the ship emissions. As pointed out by Kasibhatla et al. and Davis et al., there might be several reasons for the tendency of overestimation of modeled NO_x values found in former studies and partly in this study. There is a general need for more observational data in order to do consistent comparisons. Overestimation of the ship emissions in certain areas cannot be ruled out. The model handling of NO_y chemistry, especially the possibility of formation in plume processes can be important [*Kasibhatla et al.*, 2000; *Davis et al.*, 2001].

[73] In addition to participating in the ozone-producing cycle, NO_x oxidation will contribute to acidification in the form of HNO_3 formation (reaction (R7)). We observe a large seasonal variation in the surface ozone perturbation, which partly reflects changes in the NO_x distribution and

Table 15. Comparison of Modeled and Measured NO_y and of NO_x[a]

Component	Observed Medians	Model Without Ship Emissions	Model With Ship Emissions
NO_y	262	182	270
NO_x	12	26.5	68.7

[a]Data taken from *Kasibhatla et al.* [2000].

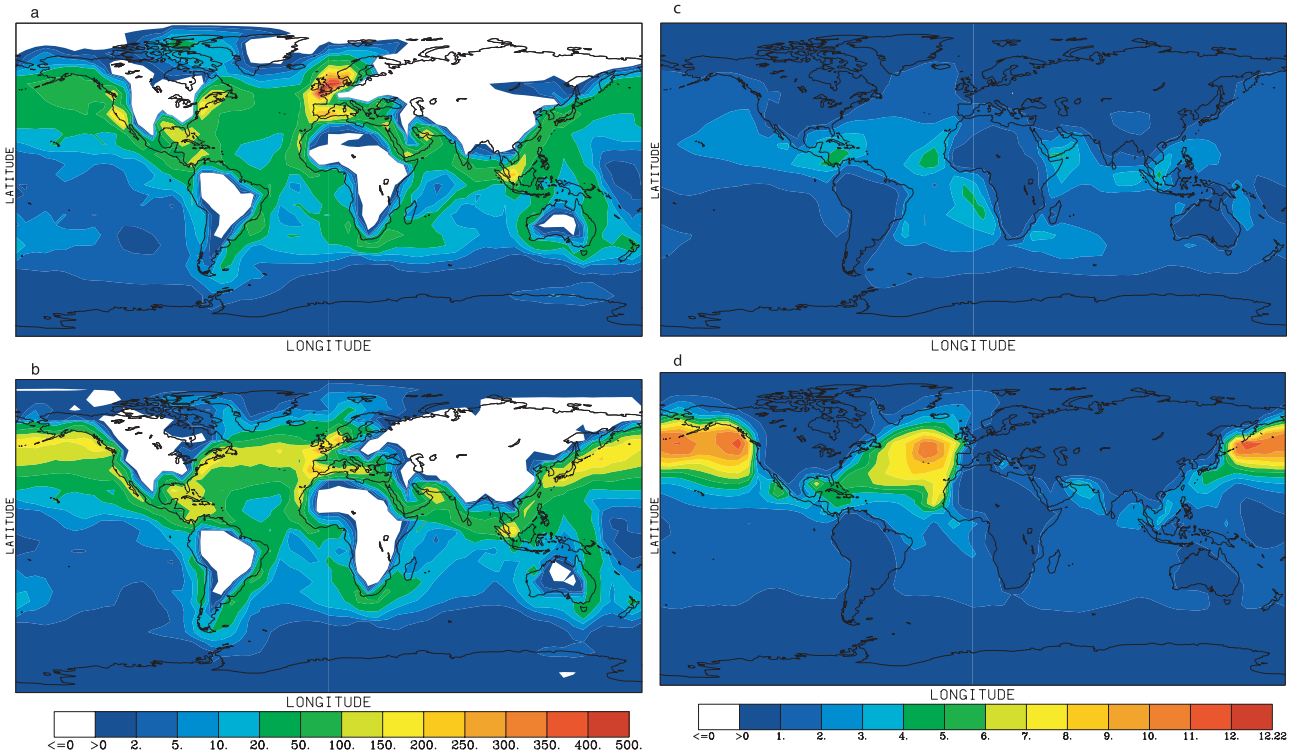

Figure 10. Absolute difference in monthly mean NO_x (ppt) for (a) January and (b) July and in monthly mean ozone (ppb) for (c) January and (d) July in the first model layer, for a run with and without CO and NO_x emissions from ship using the AMVER distribution. NO_x emission patterns are clearly dependent upon both meteorological conditions and variations in emissions. The seasonal ozone response is dependent on emissions, meteorology, and solar radiation.

partly changes in chemical activity initiated by seasonal changes in solar radiation. We find the largest ozone perturbation over remote oceans where pollution levels are low and ozone production is efficient. This feature is very different from the NO_x perturbations (Figure 10b), which often are high in more polluted coastal regions. The largest perturbations are found in July with surface ozone perturbations exceeding 10 ppb in regions of the Atlantic Ocean and the Pacific Ocean at northern midlatitudes. This is almost a doubling of the background ozone levels given in Figures 9a and 9b. In January with low chemical activity at northern latitudes, the perturbations are shifted more to the south with maximum perturbations on the order of 3–4 ppb. In the Atlantic the increase off the coast of West and Southeast Africa is enhanced with up to 25%. In the Northern Hemisphere perturbations are much smaller. In the free troposphere the ozone perturbations are smaller than in the boundary layer, but cover a larger area, since the ozone lifetime is longer.

6.5. Sulfur Perturbation From Ship Emissions

[74] Oslo CTM2 results indicate that about 46% of the SO_2 emitted to the atmosphere is lost by dry deposition (the wet deposition is negligible). The remaining part is oxidized to sulfate either by OH in the gas phase or heterogeneously by O_3, H_2O_2, HO_2NO_2, or metals (inside clouds). For the in-cloud oxidation the scheme described by *Jonson et al.* [2000b] is applied. This determines modified reaction rates, based on meteorological cloud data (cloud water content, cloud fraction), Henry's law constants, equilibrium rates, and gas phase reaction rates. SO_2 and sulfate (SO_4^{2-}) are important in two aspects; first concerning the acidification, i.e., dry and wet deposition of sulfur. Second, it has a climate effect; a direct effect where sulfate particles reflect incoming solar radiation and an indirect effect where the increased number of particles affects the formation of clouds. The lifetime of SO_2 is short, with a lifetime of 1 day, well within the 0.5–2 days range found in the literature. The fields of SO_2 are dominated by the anthropogenic emissions in the Northern Hemisphere. The fields of sulfate resemble the fields of SO_2 but are somewhat enlarged and downstream because of a time lag before SO_2 is oxidized to sulfate. Figure 11a shows global sulfate distribution from all sources in January in the lowermost layer with high concentrations in the Northern Hemisphere, especially in China. The largest effect from ship emissions is found close to the sources, i.e., in ports and along the trade routes. Geographically, the largest effect is seen in the western US, Mexican Gulf, and off the East coast of the US, along the west coast of Europe and Africa and in Indonesia, a pattern similar to, e.g., *Capaldo et al.* [1999]. Most of the sulfur emitted from ships is deposited over oceans due to the high dry deposition velocity of SO_2 over water surfaces. However some of the SO_2 will reach land, especially over Europe where the emissions occur to the west of the continent and the westerly winds will transport the sulfur toward land. The relative yearly average contribution to sulfur deposition from ship emissions, using the AMVER

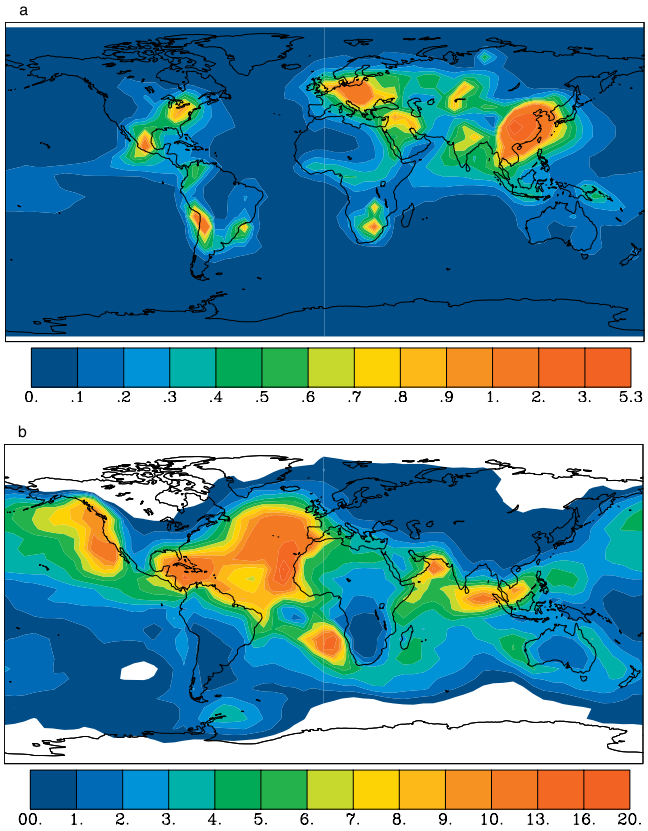

Figure 11. (a) Monthly averaged sulfate in the lowermost layer for January (unit ppb). Anthropogenic emission inventory is for 1996. In the Northern Hemisphere maximum is found in China due to the high anthropogenic emissions and low abundance of oxidants. Emissions. (b) Relative increase (given in %) in yearly average wet deposition of sulfate due to ship emissions (AMVER: no ship).

data, is depicted in Figure 11b. The largest relative increase in sulfate deposition is found over oceans where emissions occur, and where sulfate levels from other sources are low. However, sulfur emissions from ship also have an impact on coastal regions in Europe (Spain, France, Ireland), the US and Southern Asia. Typical increases in the acidification in these regions are in the range 3–10%.

[75] The AMVER emission inventory gives an increase in the total global aerosol loading of sulfate of 2.9% due to ship emissions, but in some areas (North Atlantic and the west coast of Europe) the abundance of sulfate (total column) increases by up to 8%.

[76] We did a sensitivity test using the COADS emission inventory (results not shown) comprising much larger SO_2 emissions over the North Sea than the AMVER emissions. Compared to the AMVER emissions the COADS emissions lead to a substantial increase (~12%) in both the aerosol loading and wet deposition of sulfate over southern Scandinavia and Germany. The largest effect was seen in January. Elsewhere, the use of COADS emissions gave smaller effect than the AMVER emissions.

Table 16. Relative Changes of Global Yearly Averaged OH Concentrations and Methane Lifetime Compared to a Simulation Without Ship Emissions

Simulation	Ship Emission Components Included	OH Change, %	CH_4 Lifetime Change, %
COADS	CO, NO_x	+2.22	−3.23
PF	CO, NO_x	+2.18	−2.81
AMVER	CO, NO_x	+3.01	−4.22
AMVER+	CO, NO_x,CH_4,VOC	+2.96	−4.19

6.6. Changes in Methane Caused by Ship Emissions

[77] A secondary effect of the emissions of pollutants to the atmosphere is the change in OH and thereby changes in methane concentrations (reactions (R1)–(R6)). The emission of NO_x from ship will in general enhance OH (Table 16) and thereby reduce methane lifetime. The dependency of OH on ambient NO_x levels follow a similar nonlinearity as that already discussed for ozone. This means that regional effects sometimes tend to be larger than the average values given in Table 16. In highly polluted areas the emissions from ship results in OH reductions during wintertime. In the low NO_x regimes found over most of the oceans the ship emissions of CO and VOCs will reduce OH. However, as can be seen from Table 16 the effects of including methane and VOCs emissions from ships seem to give minimal effect on the global-averaged OH and methane levels. For the simulations using the AMVER distributions, the global-averaged OH increase due to ship emissions is about 3% and the decrease in methane lifetime about 4.2%. If we take into account a chemical feedback factor of 1.4 due to the impact of methane change on its own lifetime, ship emissions lead to an increase in methane equilibrium values of

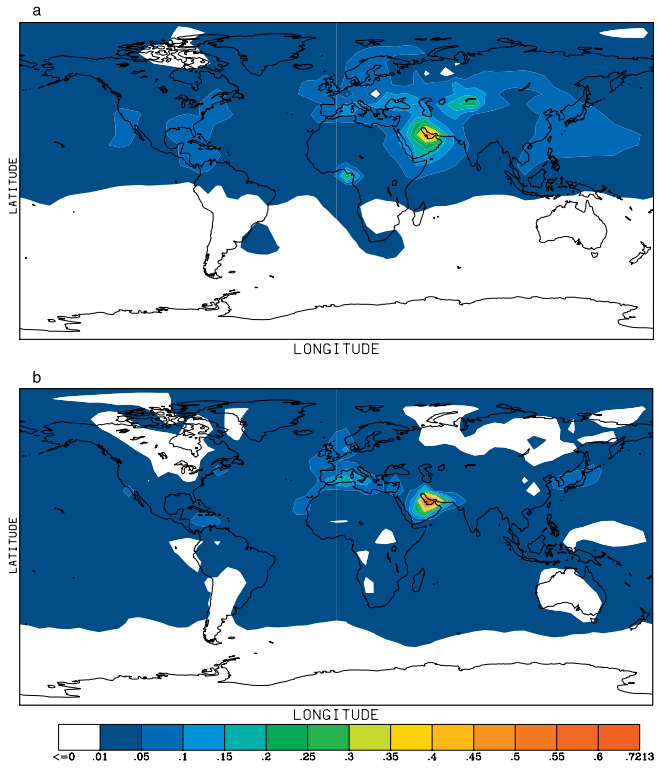

Figure 12. The monthly averaged ozone difference (in ppb) for (a) January and (b) July, is shown comparing a run with ship emissions including VOC and CH_4 and one with only CO and NO_x emissions.

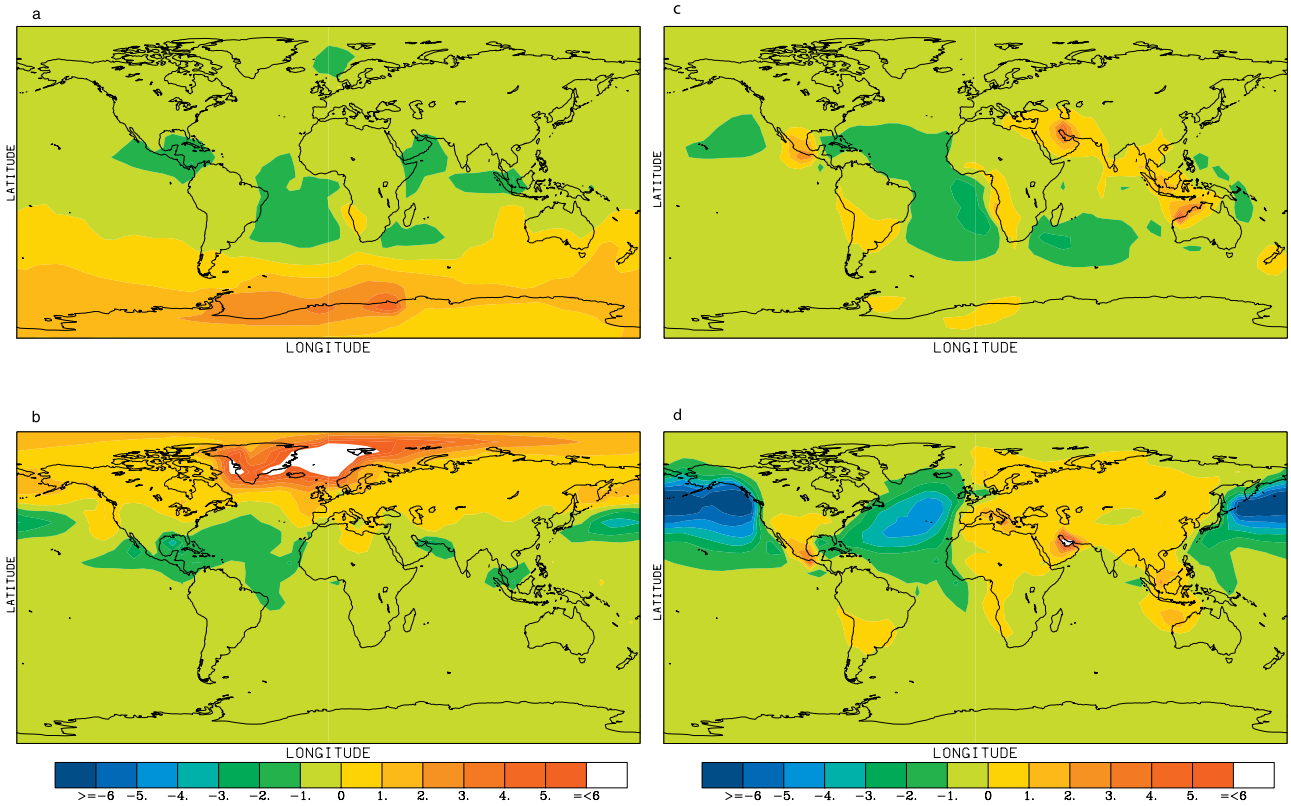

Figure 13. The absolute difference in ozone values between the COADS and AMVER distributions for (a) January and (b) July and between the PF and AMVER distributions for (c) January and (d) July.

5.5–6%. This significant change reflects the quite effective increase in OH production when NO_x levels are raised over relatively remote oceanic areas with low background values. The numbers obtained here are slightly larger than the changes in methane lifetime obtained by *Lawrence and Crutzen* [1999]. They obtained a reduction in methane lifetime from 9.6 to 9.2 years. The AMVER distributions have the most uniform dispersion of the emissions and therefore give the largest global-averaged OH increase. Due to the temperature dependency of reaction (R6), the changes in methane lifetime are very sensitive to OH changes at low latitudes and altitudes. The AMVER distribution also results in slightly larger emissions in tropical areas (Figures 5 and 6) compared to PF and COADS. Since the global-averaged OH increase also is largest for the AMVER distribution, AMVER also gives the largest global-averaged reduction in methane lifetime. Dividing the relative change in methane with the relative change in OH (Table 16), COADS is the most efficient in reducing the methane lifetime. Although the changes in OH are moved to higher latitudes with this distribution, the OH changes are more confined to the lower troposphere due to less efficient vertical transport. During the summer season with high temperatures and high OH values, methane is lost at a higher rate than during other seasons.

6.7. Ozone Response to VOC and Methane Emissions

[78] The ozone perturbation from ship emissions described above includes only the CO and NO_x emissions. The effect on ozone when VOC and methane emissions are included in the model runs is shown in Figure 12. Adding these emissions gives only a very small global increase. Increase in ozone seen in the main crude oil ports is due to emissions of VOC. The increase is less than 1 ppb in the areas of maximum impact (the Arabic peninsula). It therefore appears that adding methane and VOC emissions to the emissions of NO_x and CO from ship has only a small impact on the large-scale ozone levels.

6.8. Differences in Ozone Response Between AMVER and COADS and PF

[79] We have used the Global CTM to study differences in the chemical response in the atmosphere to different distributions in the three emission inventories AMVER, COADS, and PF. The amount of emitted gases in the rural and background areas is important for the model simula-

Table 17. Calculations, Global Average Change in Concentrations and RF Due to Ship Emissions

Climate Compound	Changes Due to Ship Emission	RF Due to Ship Emission, W/m^2	Total RF Since Preindustrial Time, W/m^2
CO_2	2%	0.030	1.46
O_3	0.7 DU[a]	0.029	0.35
CH_4	−4.2% (5.9[b])	−0.020 (−0.28[b])	0.48
Sulfate	2.9%	−0.020	−0.40

[a]1 DU = 1 Dobson Unit (2.7×10^{16} molecules/cm^2). The estimated ozone is from surface up to 323 hPa.
[b]The number has a feedback factor (impact of ozone changes on its own lifetime) of 1.4 included.

tions. COADS has more emission at high latitudes than AMVER. Figure 13a shows the difference in modeled ozone distribution using the two emission inventories. Generally, the difference in ozone is highest at high latitudes in the summer hemisphere. This is related to the differences in the background distribution of NO_x. Some of the NO_x emitted by COADS at high latitudes is temporarily stored as the longer-lived nitrogen compounds PAN and HNO_3 and transported into polar regions. During summer when sunlight is present and temperatures are higher these components are recycled back to NO_x. At middle and low latitudes the response is a slight reduction of ozone in the COADS run compared to the AMVER run and can probably be attributed to lower NO_x emissions in the regions that have NO_x limited chemistry.

[80] In Figure 13b we can see that there are significant differences in the ozone response between the PF and AMVER distribution. Less NO_x and CO are emitted over open sea and more is emitted while the ships are in coastal regions in the PF inventories. The ozone reduction is more than 5 ppb over the Atlantic and the Pacific in July.

6.9. Estimated Radiative Forcing

[81] Emissions of pollutants from ship contribute both positively and negatively to the overall RF. Emissions of CO_2 and the generation of ozone from NO_x emissions give positive contributions to RF, while formation of sulfate from SO_2 emissions and enhanced loss of methane give a negative contribution to RF. Table 17 shows estimated global average changes in the distribution and the contribution to radiative forcing from the individual climate compounds. Current estimates of the total radiative forcing since preindustrial time are also included in the figure. The calculations show that the impact of NO_x emissions from ship on RF, through perturbation of ozone and methane, nearly cancel out which has been demonstrated previously for emissions from other surface sources [*IPCC*, 1996]. Since the positive RF from CO_2 is significantly larger than the negative RF from sulfate the total RF is small but positive, approximately $0.01-0.02$ W/m^2. The numbers are connected with significant uncertainties. It is interesting to notice that contribution to RF from the different climate compounds from global ship emission as well as the total RF is similar to the contribution from global air traffic [*IPCC*, 1996]. It should also be noted that the contribution from sulfate and other particles through indirect effects are not included. *Capaldo et al.* [1999] estimated the indirect effect from ship traffic through sulfate and organic particles, and found an RF of -0.1 W/m^2, which is significantly larger than the direct sulfate effect obtained in this study. However, we should recognize that studies of indirect effects are very uncertain; *IPCC* [1996] does not give a number, but a wide uncertainty range (0 to 2 W/m^2) for the total global indirect aerosol effect.

[82] The total RF (Table 17) for the different climate compounds is taken from *IPCC* [1996]. For CO_2, CH_4, and sulfate calculated RF is scaled based on the percentage change. For sulfate and also for CH_4, which have relatively short lifetimes, these should be valid assumptions. For CO_2 with a long lifetime, the assumption implies that increases over past decades in ship emissions have been similar to the increase in CO_2 emissions. For O_3 a scaling factor of 0.042 (W/m^2/DU) is used [*IPCC*, 1996].

7. Conclusions

[83] Ship-type specific engine modeling shows that the cargo and passenger fleet in international trade consumes the majority of the marine bunker sold to the world fleet of ocean-going vessels. Emission from bunker fuel burned by the international cargo and passenger fleet represents a significant contribution to the global anthropogenic emissions, and particularly, for NO_x and SO_x. The majority of the emissions occur in Northern Hemisphere within a fairly well-defined system of international sea routes. The most accurate geographical representations of the emissions are obtained using a method based on the relative reporting frequency weighted by the ship size. The different modeling approaches show good agreement with regard to the annual fuel consumption for crude oil carriers.

[84] The model calculations have shown that the response in the atmospheric chemical composition from ship emission is rather complex, and does not reflect the pattern of emissions. Added to this, is the uncertainty associated with plume effects that might reduce the available NO_x from the ship emissions. Due to the highly nonlinear response in ozone formation from emissions of precursors like CO and NO_x, with higher efficiency in regions that are affected little by pollutants, ozone formation due to ship emissions over oceans away from industrial regions like the Atlantic and Pacific Oceans are more efficient than emissions over polluted coastal regions (e.g., the North Sea). We also find that the formation of secondary pollutants and climate compounds such as ozone and sulfate shows large seasonal variations at middle and high northern latitudes due to the large seasonal variation in chemical activity. Furthermore, secondary pollutants are transported over rather large areas leading to enhanced levels well outside the traffic corridors. In parts over the Atlantic and Pacific Oceans, ozone levels are significantly enhanced by ship emissions. The oxidation capacity of the atmosphere (through the effect on the OH distribution) is enhanced by ship emissions, leading to increased rate of methane loss and reduced concentrations. A consequence of this is that RF from NO_x-induced changes in ozone and methane is close to zero, and the total RF is small due to several canceling effects. Coastal regions in the vicinity of major ship tracks are affected by sulfur emissions from ship. In some coastal regions the relative deposition of sulfate is enhanced by $3-10\%$.

[85] Solutions to problems with acidification and climate change seems to require different approaches. The impact on ozone, from a climate point of view, can be reduced by lowering the NO_x emissions in oceanic background regions, while NO_x reduction is much less effective in reducing ozone in the coastal areas with high background NO_x levels like in the North Sea, as discussed in section 6.4. The situation is opposite for the acidification problem where reductions in coastal and in-port areas are more important than reduction in open sea. Moreover, the political tools to impose regulations on international shipping are few. This is also illustrated by the fact that the IPCC did not include ship emissions in the Kyoto protocol.

[86] **Acknowledgments.** The preparation of this paper was cofunded by the Norwegian Research Council (contract 139305/230). We are indebted to Steve Worley of NCAR, Doug Horton, Elissa Carroll, and Travis Hessenauer of AMVER, and to Giles Whitby-Smith of PF for providing traffic data. We would also like to acknowledge the reviewers and Stephen McAdam at DNV, for significantly improving the paper.

References

Adcock, L. E., and G. A. Stitt, *AMI International's Naval Main Propulsion Market Overview*, AIM Int., Bremerton, Wash., 1995.

Benkovitz, C. M., M. T. Scholtz, J. Pacyna, L. Tarrasón, J. Dignon, E. C. Voldner, P. A. Spiro, J. A. Logan, and T. E. Graedel, Global gridded inventories of anthropogenic emissions of sulfur and nitrogen, *J. Geophys. Res.*, *101*, 29,239–29,253, 1996.

Berntsen, T., and I. S. A. Isaksen, A global three-dimensional chemical transport model for the troposphere: 1. Model description and CO and ozone results, *J. Geophys. Res.*, *102*, 21,239–21,280, 1997.

Brasseur, G. P., D. A. Hauglustaine, S. Walters, P. J. Rasch, J.-F. Müller, C. Granier, and X. X. Tie, MOZART, a global chemical transport model for ozone and related chemical tracers: 1. Model description, *J. Geophys. Res.*, *103*, 28,265–28,289, 1998.

Calhoun, D. R., (Ed.), Events of 1998: Military Affairs, in *1999 Britannica Book of the Year*, pp. 278–281, Encycl. Br., Chicago, Ill., 1999.

Capaldo, K., J. J. Corbett, P. Kasibhatla, P. S. Fischbeck, and S. N Pandis, Effects of ship emission on sulphur cycling and radiative climate forcing over the ocean, *Nature*, *400*, 743–746, 1999.

CONCAWE, The contribution of sulphur dioxide emission from ships to coastal deposition and air quality in the channel and southern North Sea area, *Rep. 2/94*, Brussels, 1994.

Cooper, D. A., K. Peterson, and D. Simpson, Hydrocarbons, PAH, and PCB emissions from ferries: A case study in the Skagerak-Kattegatt-Oresund region, *Atmos. Environ.*, *30*(14), 2463–2473, 1996.

Corbett, J. J., and P. S. Fischbeck, Emissions from waterborne commerce vessels in United States continental and inland waterways, *Environ. Sci. Technol.* [*Washington D. C.*], *34N*, 3254–3260, 2000.

Corbett, J. J., P. S. Fischbeck, and S. N. Pandis, Global nitrogen and sulfur inventories for oceangoing ships, *J. Geophys. Res.*, *104*, 3457–3470, 1999.

Cullen, W. P., Marine fuels—Worldwide sulphur levels, Det Norske Veritas Petr. Serv. Inc., Oslo, Norway, 16 Sept. 1997.

Davis, D. D., G. Grodzinsky, P. Kasibhatla, J. Crawford, G. Chen, S. Liu, A. Bandy, D. Thornton, H. Guan, and S. Sandholm, Impact of ship emissions on marine boundary layer NO_x and SO_2 distributions over the Pacific Basin, *Geophys. Res. Lett.*, *28*(2), 235–238, 2001.

Endresen, Ø., and E. Sørgård, Reference values for ship pollution, *Rep. 99-2034*, Det Norske Veritas, Oslo, 1999.

Endresen, Ø., A. Mjelde, T. Sverud, and E. Sørgård, Data and models for quantification of ship pollution, *Rep. 98-2059*, Det Norske Veritas, Oslo, 1999.

Environmental Protection Agency (EPA), VOC emission factors, AP-42, in *Transportation and Marketing of Petroleum Liquids*, vol. 1, 5th ed., pp. 5.2-1–5.2-17, Washington, D. C., 1995.

Environmental Protection Agency (EPA), Energy, in *Inventory of U.S. Greenhouse Gas Emissions and Sinks: 1990–1997*, *Rep. 236-R-99-003*, pp. 2–36, Washington, D. C., 1999.

Environmental Protection Agency (EPA), Analysis of commercial marine vessels emission and fuel consumption data, office of transportation and air quality, *Rep. 420-R-00-002*, Washington, D. C., 2000.

Environmental Protection Agency (EPA), SPECIATE, EPA's respository of total organic compound (TOC) and particulate matter (PM) speciated profiles for a wide variety of sources, visited spring 2002.

European Monitoring and Evaluation Programme (EMEP)/CORINAIR, EMEP co-operative programme for monitoring and evaluation of the long range transmission of air pollution in Europe: The core inventory of air emissions in Europe (CORINAIR), in *Atmospheric Emission Inventory Guidebook*, 2nd ed., Eur. Environ. Agency, Copenhagen, 1999.

Fearnleys, *World Bulk Trades 1997, An Analysis of 1996 With 1997 Update*, Fearnresearch, Oslo, 1997.

Fearnleys, *Review 2001* (*The Tanker and Bulk Markets and Fleets*), Fearnresearch, Oslo, 2002.

Graf, H.-F., J. Feichter, and B. Langmann, Volcanic sulfur emissions: Estimates of source strength and its contribution to the global sulfate distribution, *J. Geophys. Res.*, *102*, 10,727–10,738, 1997.

Harrington, R. L., *Marine Engineering*, 53 pp., Soc. of Nav. Archit. and Mar. Eng., Jersey City, N. J., 1992.

Hesstvedt, E., Ø. Hov, and I. S. A. Isaksen, Quasi steady-state approximation in air pollution modelling: Comparison of two numerical schemes for oxidant prediction, *Int. J. Chem. Kinet.*, *X*, 971–994, 1978.

Holtslag, A. A. M., et al., A high resolution air mass transformation model for short-range weather forecasting, *Mon. Weather Rev.*, *118*, 1561–1575, 1990.

Hough, A. M., Development of a two-dimensional global tropospheric model: Model chemistry, *J. Geophys. Res.*, *96*, 7325–7362, 1991.

Institute of Shipping Economics and Logistics (ISL), *Shipping Statistics Yearbook 1997*, edited by M. Zachcial and C. Heideloff, Bremen, Germany, 1997.

Intergovernmental Panel on Climate Change (IPCC), *Climate Change 2001: The Scientific Basis*, edited by J. T. Houghton et al., Cambridge Univ. Press, New York, 1996.

International Energy Agency (IEA), *Oil Information 2001*, edited by M. Reece, Paris, 2001.

International Energy Agency (IEA), *International Bunker Statistics Year 1996/2000*, Paris, 2003.

International Maritime Organisation (IMO), Regulations for the prevention of air pollution from ships and NO_x technical code, *ANNEX VI of MARPOL 73/78*, London, 1998.

Isaksen, I. S. A., Ø. Hov, and E. Hesstvedt, Ozone generation over rural areas, *Environ. Sci. Technol.*, *12*, 1279–1284, 1978.

Japan, A point of view toward GHG emission reduction: Preliminary study on estimation and future trend of GHG emissions from all marine vessels, *Rep. MEPC 45/INF.27*, Int. Mar. Organ., London, 10 Aug. 2000.

Jonson, J. E., L. Tarrason, and J. Bartnicki, Effects of international shipping on European pollution levels, *EMEP/MSC-W Note 5/2000*, Norw. Meteorol. Inst., Oslo, 2000a.

Jonson, J. E., A. Kylling, T. K. Berntsen, I. S. A. Isaksen, C. S. Zerefos, and K. Kourtidis, Chemical effects of UV fluctuations inferred from total ozone and tropospheric aerosol variations, *J. Geophys. Res.*, *105*, 14,561–14,574, 2000b.

Kasibhatla, P., et al., Do emissions from ships have a significant impact on concentrations of nitrogen oxides in the marine boundary layer?, *Geophys. Res. Lett.*, *27*(15), 2229–2233, 2000.

Kettle, A. J., et al., A global database of sea surface dimethylsulfide (DMS) measurements and a procedure to predict sea surface DMS as a function of latitude, longitude, and month, *Global Biogeochem. Cycles*, *13*, 399–444, 1999.

Klokk, S. N., The Norwegian Green Ship Program—Low emission diesel engines, paper presented at the Advanced Study Workshop, Air Pollut. From Mar. Eng., Athens, 20 Jan., 1994.

Lawrence, M. G., and P. J. Crutzen, Influence of NO_x emissions from ships on tropospheric photochemistry and climate, *Nature*, *402*, 167–170, 1999.

Liberia, Untitled, *Rep. MEPC 38/INF.12*, Int. Mar. Organ., London, 17 April 1996.

Liss, P. S., and L. Merlivat, Air-sea gas exchange rates: Introduction and synthesis, in *The Role of Air-Sea Exchange in Geochemical Cycling*, edited by P. Buat-Ménard, pp. 113–127, D. Reidel, Norwell, Mass., 1986.

Lloyd's Register of Shipping (LR), *Marine Exhaust Emissions Research Programme*, Lloyd's Regist. Eng. Serv., London, 1995.

Lloyd's Register of Shipping (LR), *World Fleet Statistics*, 1996, Lloyd's Regist. Eng. Serv., London, 1996.

Lloyd's Register of Shipping (LR), Marine exhaust emissions quantification study—Baltic Sea, *Rep. 98/EE/7036*, Lloyd's Regist. Eng. Serv., London, 1998.

Lloyd's Register of Shipping (LR), Marine exhaust emissions quantification study—Mediterranean Sea, *Rep. 99/EE/7044*, Lloyd's Regist. Eng. Serv., London, 1999a.

Lloyd's Register of Shipping (LR), *Lloyd's Maritime Atlas of Ports and Shipping Places*, 20th ed., Lloyd's Regist. Eng. Serv., London, 1999b.

Lloyd's Register of Shipping (LR), *World Fleet Statistics*, 2000, Lloyd's Regist. Eng. Serv., London, 2000.

Martens, O., Solutions to hydrocarbon gas emission from tankers, marine system design and operations, paper presented at ICMES 93: Marine system design and operation symposium, Inst. Mar. Eng., Hamburg, Germany, 29 Sept. to 1 Oct., 1993.

Müller, J.-F., Geographical distribution and seasonal variation of surface emissions and deposition velocities of atmospheric trace gases, *J. Geophys. Res.*, *97*, 3787–3804, 1992.

Norway, Untitled, *Rep. BCH 24/INF.28*, Int. Mar. Organ., London, 29 July 1994.

Norwegian Maritime Directorate, *List of Norwegian Vessels 1999*, Elanders Publ. AS, Oslo, 2000.

Norwegian Shipowner Association, *Quarterly Information on Shipping and Offshore Activity* (in Norwegian), vol. 4, Oslo, 2000.

Norwegian Shipowner Association, Ratio between gross tonnage/net tonnage/deadweight—Approximate conversion figures, Oslo, 2002.

Oil Industry International Exploration and Production Forum, Methods for estimating atmospheric emissions from E&P operations, *Rep. HN88-001*, London, 1993.

Olivier, J. G. J., A. F. Bouwman, C. W. M. Van der Maas, J. J. M. Berdowski, C. Veldt, J. P. J. Bloos, A. J. H. Visschedijk, P. Y. J. Zandveld, and J. L. Haverlag, Description of EDGAR version 2.0, *rep. 771060 002/ TNO-MEP, rep. R96/119*, Natl. Inst. of Public Health and the Environ., Bilthoven, Netherlands, 1996.

Organisation for Economic Co-operation and Development (OECD), *What Markets are There for Transport by Inland Waterways?*, Econ. Res. Cent., Paris, 1997.

Plass-Dulmer, C., A. Khedim, R. Koppmann, F. J. Johnen, J. Rudolph, and H. Kuosa, Emissions of light nonmethane hydrocarbons from the Atlantic into the atmosphere, *Global Biogeochem. Cycles*, *7*, 211–228, 1993.

Prather, M. J., Numerical advection by conservation of second-order moments, *J. Geophys. Res.*, *91*, 6671–6681, 1986.

Price, C., J. Penner, and M. Prather, NO_x from lightning: 1. Global distribution based on lightning physics, *J. Geophys. Res.*, *102*, 5241–5929, 1997a.

Price, C., J. Penner, and M. Prather, NO_x from lightning, 2, Constraints from the global atmospheric electric circuit, *J. Geophys. Res.*, *102*, 5251–5943, 1997b.

Singh, H. B., D. O'Hara, D. Herlth, W. Sachse, D. R. Blake, J. D. Bradshaw, M. Kanakidou, and P. J. Crutzen, Acetone in the atmosphere: Distribution, sources, and sinks, *J. Geophys. Res.*, *99*, 1805–1819, 1994.

Skjølsvik, K. O., A. B. Andersen, J. J. Corbett, and J. M. Skjelvik, Study on greenhouse gas emissions from ships, *MT Rep. Mtoo A23-038*, MARINTEK, Trondheim, Norway, 2000.

Spiro, P. A., D. J. Jacob, and J. A. Logan, Global inventory of sulfur emissions with $1° \times 1°$ resolution, *J. Geophys. Res.*, *97*, 6023–6036, 1992.

Streets, D. G., et al., The growing contribution of sulfur emissions from ships in Asian waters 1988–1995, *Atmos. Environ.*, *24*(26), 4425–4439, 2000.

Tiedtke, M., A comprehensive mass flux scheme for cumulus parameterisation on large scale models, *Mon. Weather Rev.*, *117*, 1779–1800, 1989.

United Kingdom, International collaborative FSA study—Crew performance and voyage cycles, *Rep. MSC 76/INF.6*, Int. Mar. Organ., London, 30 Aug. 2002.

United Nations, *1996 Energy Statistics Yearbook*, New York, 1998.

Whall, C., et al., Quantification of emissions from ships associated with ship movements between ports in the European Community, *Rep. 06177.02121*, Entec, Northwich, England, 2002.

Wijnolst, N., and T. Wergeland, *Shipping*, Delft Univ. Press, Delft, Netherlands, 1997.

Wild, O., X. Zhu, and M. J. Prather, Fast-J: Accurate simulation of in- and below cloud photolysis in tropospheric chemical models, *J. Atmos. Chem.*, *37*, 245–282, 2000.

Worley, S. J., *Shipping Statistics*, Natl. Cent. for Atmos. Res., Boulder, Colo., 1999.

Worley, S. J., *Information About the VOS Fleet*, Natl. Cent. for Atmos. Res., Boulder, Colo., 2001.

Worley, S. J., *Documentation That Norwegian Oil Rigs are Included as Ships*, Natl. Cent. for Atmos. Res., Boulder, Colo., 2002.

T. F. Berglen, S. B. Dalsøren, I. S. A. Isaksen, and J. K. Sundet, Department of Geophysics, University of Oslo, Box 1022, N-0315 Oslo, Norway. (t.f.berglen@geofysikk.uio.no; s.b.dalsoren@geofysikk.uio.no; i.s.a.isaksen@geofysikk.uio.no; j.k.sundet@geofysikk.uio.no)

Ø. Endresen, G. Gravir, and E. Sørgård, Det Norske Veritas, Veritasveien 1, Oslo, N-1322 Hovik, Norway. (oyvind.endresen@dnv.com; gjermund.gravir@dnv.com; eirik.sorgard@kpb.no)